The Journal of Toxicological Sciences (J. Toxicol. Sci.)
Vol.33, No.4, 405-413, 2008

Original Article

Regulation of insulin-like growth factor binding protein-1 and lipoprotein lipase by the aryl hydrocarbon receptor

Keiichi Minami[1], Miki Nakajima[1], Yuto Fujiki[1], Miki Katoh[1], Frank J. Gonzalez[2] and Tsuyoshi Yokoi[1]

[1]Drug Metabolism and Toxicology, Division of Pharmaceutical Sciences, Graduate School of Medical Science, Kanazawa University, Kanazawa 920-1192, Japan
[2]Laboratory of Metabolism, National Cancer Institute, Bethesda, MD 20892, USA

(Received April 21, 2008; Accepted May 10, 2008)

ABSTRACT — The aryl hydrocarbon receptor (Ahr), a ligand-activated transcriptional factor, mediates the transcriptional activation of a battery of genes encoding drug metabolism enzymes. In the present study, we investigated the hepatic mRNA expression profile in *Ahr*-null (*Ahr* KO) mice compared to wild-type mice by microarray analysis to find new Ahr target genes. Pooled total RNA samples of liver extracted from 7- and 60-week-old *Ahr* KO or wild-type mice were studied by DNA microarray representing 19,867 genes. It was demonstrated that 23 genes were up-regulated and 20 genes were down-regulated over 2 fold in *Ahr* KO mice compared with wild-type mice commonly within the different age groups. We focused on insulin-like growth factor binding protein-1 (Igfbp-1) and lipoprotein lipase (Lpl) that were up-regulated in *Ahr* KO mice. The higher expression in *Ahr* KO mice compared to wild-type mice were confirmed by real-time RT-PCR analysis. In the wild-type mice but not in the *Ahr* KO mice, 2,3,7,8-tetrachlorodibenzo-*p*-dioxin (TCDD) treatment increased the Igfbp-1 and Lpl mRNA levels. The expression profile of Igfbp-1 protein was consistent with that of Igfbp-1 mRNA. Since Lpl is the primary enzyme responsible for hydrolysis of lipids in lipoproteins, the serum triglyceride levels were determined. Indeed, the serum triglyceride levels in *Ahr* KO mice was lower than that in wild-type mice in accordance with the Lpl mRNA levels. Contrary to our expectation, TCDD treatment significantly increased the serum triglyceride levels in wild-type, but did not in *Ahr* KO mice. These results suggest that serum triglyceride levels are not correlated with hepatic Lpl expression levels. In the present study, we found that Ahr paradoxically regulates Igfbp-1 and Lpl expressions in the liver.

Key words: Aryl hydrocarbon receptor, Knockout mice, Igfbp-1, Lpl

INTRODUCTION

Aryl hydrocarbon receptor (Ahr) is a ligand-activated transcription factor and a member of the basic helix-loop-helix/Per-Arnt-Sim (bHLH/PAS) family of chemosensors and developmental regulators. Various kinds of environmental stimuli including 2,3,7,8-tetrachlorodibenzo-*p*-dioxin (TCDD) are well known as ligands of Ahr (Schmidt and Bradfield, 1996; Sogawa and Fujii-Kuriyama, 1997). Upon binding to the ligand, Ahr translocates to the nuclei, coincident with formation of a heterodimeric complex with Ahr nuclear translocator (Arnt). The ligand-activated Ahr mediates the transcriptional activation of a battery of genes encoding enzymes such as cytochrome P450 (CYP) 1 family, NAD(P)H: quinone oxidoreductase and glutathione *S*-transferase Ya subunit that function in the metabolism of xenobiotics and endobiotics (Bock, 1994; Rowlands and Gustafsson, 1997).

Gene knockout technology is a useful tool to estimate the roles of certain genes *in vivo*. *Ahr*-null (*Ahr* KO) mice on a C57BL/6 strain background were established by three research groups (Fernandez-Salguero *et al.*, 1995; Schmidt *et al.*, 1996; Mimura *et al.*, 1997). The *Ahr* KO mice established by Fernandez-Salguero *et al.* (1995) exhibited 40-50% neonatal lethality, although survivors reached maturity and were fertile. The *Ahr* KO mice established by the latter two groups exhibited no neonatal lethality, but the growth rate was decreased in the first few weeks. In the *Ahr* KO mice, the size of the liver has been reported to be decreased compared with

Correspondence: Tsuyoshi Yokoi (E-mail: tyokoi@kenroku.kanazawa-u.ac.jp)

that in wild-type mice (Fernandez-Salguero *et al.*, 1995; Schmidt *et al.*, 1996). Hepatic portal fibrosis and hepatic vascular hypertrophy were observed in the *Ahr* KO mice (Fernandez-Salguero *et al.*, 1995; Fernandez-Salguero *et al.*, 1997). In addition, the accumulation of retinoid in the liver owing to reduced retinoic acid metabolism has also been documented (Andreola *et al.*, 1997). The abnormality of retinoid homeostasis was considered to be the reason for the liver fibrosis in the *Ahr* KO mice (Andreola *et al.*, 2004). Zaher *et al.* (1998) found that transforming growth factor β is overexpressed in the liver of *Ahr* KO mice, and this could be a causal factor of liver fibrosis. Thus, these findings suggest that Ahr expression in the liver is important for normal liver development. In the present study, we sought to determine the hepatic mRNA expression profile in *Ahr* KO mice compared with that in wild-type mice by microarray analysis to identify new targets of Ahr.

MATERIALS AND METHODS

Chemicals

CodeLink™ Expression Assay Reagent kit, Manual Prep and streptavidin-Cy5 were purchased from GE Healthcare Bio-Sciences (Piscataway, NJ, USA). QIAquick PCR Purification Kit and RNeasy Mini Kit were from Qiagen (Hilden, Germany). NEN Blocking Reagent and Biotin 11-UTP were from Perkin-Elmer Life Sciences (Boston, MA, USA). ReverTra Ace (Moloney Murine Leukemia Virus Reverse Transcriptase RNase H Minus) was from Toyobo (Osaka, Japan). SYBR Premix Ex Taq (Perfect Real Time) was from Takara (Shiga, Japan). Goat anti-mouse insulin-like growth factor binding protein 1 (Igfbp-1) antibody was purchased from Santa Cruz Biotechnology (Santa Cruz, CA, USA). Triglyceride E Test Wako was from Wako Pure Chemical Industries (Osaka, Japan). TCDD was from Cambridge Isotope Laboratories (Cambridge, MA, USA). All primers were commercially synthesized at Hokkaido System Sciences (Sapporo, Japan). Other chemicals were of the highest grade commercially available.

Animals and treatment

Ahr KO mice generated by Fernandez-Salguero *et al.* (1995) were used. Animals were housed in the institutional animal facility in a controlled environment (temperature 25 ± 1°C, humidity 50 ± 10% and 12 hr light/12 hr dark cycle) with access to food and water *ad libitum*. Animal maintenance and treatment were conducted in accordance with the National Institutes of Health Guide for Animal Welfare of Japan, as approved by the Institutional Animal Care and Use Committee of Kanazawa University. Genotyping of animals was carried out by polymerase chain reactions (PCRs) described previously (Takemoto *et al.*, 2004). For the DNA microarray experiment, 7- and 60-week-old *Ahr* KO and wild-type mice were used. For the TCDD treatments, TCDD in corn oil (40 μg/kg body weight per day) was intraperitoneally administered to 35-week-old *Ahr* KO mice and 14-week-old wild-type mice for four days. Corn oil (2 ml/kg body weight) was administered as a control.

Total RNA preparation

Mice were sacrificed and the livers were collected and immediately frozen in liquid nitrogen and stored at −80°C until use. Total RNA from liver was isolated using ISOGEN (Nippon Gene, Tokyo, Japan) according to the manufacturer's protocol. Equal amounts of total RNA from 5 - 7 mice were pooled.

Microarray analysis

Microarray analysis was performed using a CodeLink™ Bioarray Perfect System according to the manufacturer's protocol (GE Healthcare Bio-Sciences). A Codelink™ UniSet Mouse 20K I Bioarray (GE Healthcare Bio-Sciences) consisting of 19,867 genes including expression sequence tags (ESTs) was used. Processed slides were scanned with an Agilent G2565BA Microarray Scanner using Agilent Scan Control Software (Agilent Technologies, Palo Alto, CA, USA) with the laser set to red (633 nm) and the photomultiplier tube value to 70%. The scanned images for each slide were analyzed using CodeLink™ Expression Analysis Software (GE Healthcare Bio-Sciences). The microarray data quality control was as follows: present, no flags (neither marginal nor absent); marginal, low quality spots judged by analysis software; absent, low signal density spots. Microarray data management was performed with GeneSpring software (Agilent Technologies). Comparison of the present genes, expression filtering and experiment normalization were performed. The individual gene expression for each array was normalized to their respective median value. Expression filters included the requirement that the genes be present in over 200% of controls for up-regulated genes and below 50% of controls for down-regulated genes.

Real-time RT-PCR

Total RNA (4 μg) was reverse transcribed using ReverTra Ace according to the manufacturer's instructions and the resulting cDNA was amplified by PCR. Real-time PCR was performed using the Smart Cycler (Cepheid,

Sunnyvale, CA, USA). PCR reactions were carried out as follows: A 1 μl portion of the reverse transcribed mixture was added to a PCR mixture containing 0.4 μM of each primer and SYBR Premix Ex Taq solution in a final volume of 25 μl. The primers used for PCR are shown in Table 1. The PCR condition for *Igfbp-1*, *Lpl*, *Cyp17a1*, and *GAPDH* was as follows: after an initial denaturation at 95°C for 30 sec, the amplification was performed by denaturation at 94°C for 4 sec, annealing and extension at 64°C for 20 sec for 45 cycles. The amplified products were monitored directly by measuring the increase of the dye intensity of the SYBR Green I. To normalize RNA loading and PCR variations, the signals of targets were corrected with the signals of GAPDH mRNA as the internal standard.

Western blot analysis of Igfbp-1

Ahr KO and wild-type mice were sacrificed 24 hr after the last treatment with TCDD. The livers were homogenized with buffer (0.1 M Tris-HCl (pH 7.4), 0.1 M KCl, 1 mM EDTA, 1 mM Na_3VO_4, 1 mM NaF) and liver homogenates (100 μg protein) subjected to SDS-polyacrylamide gel electrophoresis with 10% polyacrylamide gels followed by Western blotting using a PVDF membrane (Immobilon-P, Millipore, Billerica, MA, USA). The membrane was incubated with goat anti-Igfbp-1 antibody at a dilution of 1:200. Biotinylated anti-goat IgG and a VECTASTAIN ABC kit (Vector Laboratories, Burlingame, CA) were used for diaminobenzidine staining. The quantitative analysis of protein expression was performed using ImageQuant TL software (GE Healthcare Bio-Sciences).

Serum triglycerides concentration

Blood samples were collected from the postcaval vein 24 hr after the last treatment with TCDD. The serum triglyceride concentration was measured using Triglyceride E Test Wako.

Table 1. Primers used in the present study.

Primer	Sequence
Cyp17a1 S	5'-GTA TTC AGC ACC TTT TCC CT-3'
Cyp17a1 AS	5'-AAT ATG TCC ACC AGA TCG CT-3'
IGFBP-1 S	5'-CAA ACT GCA ACA AGA ATG G-3'
IGFBP-1 AS	5'-TGT ATC AAG CAG TAT GTG G-3'
LPL S	5'-AGA AGC AGC AAG ATG TAC CT-3'
LPL AS	5'- GAA ACT TTC TCC CTA GCA CA-3'
GAPDH S	5'-AAA TGG GGT GAG GCC GGT-3'
GAPDH AS	5'-ATT GCT GAC AAT CTT GAG TGA-3'

Statistical analysis

Statistical significance was determined by analysis of variance (ANOVA) followed by Dunnett's test for multiple comparisons.

RESULTS

Comparison of gene expression profiles in Ahr KO and wild-type mice

Among 19,867 genes, 11,509 (58%) genes were categorized into 15 groups (Table 2). Among these, 7,255 (37%) genes showed sufficient spot density. In 7-week-old *Ahr* KO mice, the expression levels of 133 genes were elevated, whereas those of 95 genes were suppressed compared with age-matched wild-type mice. In 60-week-old *Ahr* KO mice, the expression levels of 76 genes were elevated, whereas those of 136 genes were suppressed compared with age-matched wild-type mice. In both 7- and 60-week-old *Ahr* KO mice, 23 genes were commonly elevated and 20 genes were commonly suppressed. The 43 common genes are shown in Table 3. Cyp1a2 and Ugt1a6, which are known to be highly regulated by Ahr, were down-regulated in *Ahr* KO mice. In addition, we found that Slc22a7 (organic anion transporter 2, Oat2) and Slc2a2 (facilitated glucose transporter 2) were also down-regulated in *Ahr* KO mice. These results suggest that these genes might be targets of Ahr regulation.

The expression levels of methylmalonyl-Coenzyme A mutase, lipoprotein lipase (Lpl), and Cyp17a1 were highly (over 10 fold in 7-week-old mice) up-regulated in *Ahr* KO mice. Among these, the spot density of Lpl was highest. We additionally found that Igfbp-1 was unexpectedly up-regulated in *Ahr* KO mice, because previous studies reported that *Igfbp-1* mRNA was induced by TCDD via Ahr activation (Adachi *et al.*, 2004, Marchand *et al.*, 2005). In a subsequent study, we investigated in detail the expression of Igfbp-1 and Lpl in the liver.

Real-time RT-PCR analysis

To confirm the results of the DNA microarray analysis, real-time RT-PCR analysis was performed (Fig. 1). The hepatic *Igfbp-1* mRNA levels in *Ahr* KO mice were 7 fold (7-week-old) and 24 fold (60-week-old) higher than those in age-matched wild-type mice. The hepatic *Lpl* mRNA levels in *Ahr* KO mice were 8 fold (7-week-old) and 3 fold (60-week-old) higher than those in age-matched wild-type mice. Thus, the differences in the expression levels detected by microarray analysis were reproducible.

Table 2. Number of genes of which expression were significantly changed in *Ahr* KO mice.

Category	Total [1]	Present [2]	Up-regulated (> 2 fold)			Down-regulated (< 2 fold)		
			7 w	60 w	7 & 60 w	7 w	60 w	7 & 60 w
Apoptosis regulator	265	198	5	3	0	0	5	0
Cancer	168	109	2	2	2	1	2	0
Cell cycle	386	252	5	3	1	0	0	0
Chaperone	429	276	4	3	0	4	9	0
Enzyme	3,829	2,615	59	28	12	54	59	11
Immunity	143	93	1	1	0	2	2	1
Microtubular	63	38	0	0	0	0	0	0
Motor	40	24	2	1	1	0	0	0
Nucleic acid binding	1,812	1,183	18	6	0	9	17	0
RNA	14	12	0	0	0	0	0	0
Signal transducer	839	387	6	6	2	7	6	1
Storage	11	5	0	0	0	0	0	0
Stractural protein	1,341	700	17	11	3	7	11	2
Transport	1,465	955	11	9	2	10	20	5
Others	704	408	3	3	1	1	5	0
	11,509	7,255	133	76	23	95	136	20

Up-regulated and down-regulated genes showed more than 200% expression and less than 50% expression, respectively, compared with those in wild type mice.

[1] Number of genes of which categories were defined.

[2] Number of genes showing enough spot density.

Effects of TCDD treatment on Igfbp-1 and Lpl mRNA expression in *Ahr* KO and wild-type mouse livers

We investigated the effect of TCDD treatment on *Igfbp-1* and *Lpl* mRNA expressions. Real-time RT-PCR analyses revealed that *Igfbp-1* mRNA was significantly (7 fold) increased by TCDD in wild-type mice, but not in *Ahr* KO mice, showing 8-fold higher *Igfbp-1* mRNA levels than those in wild-type mice (Fig. 2A). *Lpl* mRNA was also significantly (4 fold) increased by TCDD in wild-type mice, but not in *Ahr* KO mice, showing 4-fold higher *Lpl* mRNA levels than those in wild-type mice (Fig. 2B).

Igfbp-1 protein expression

Western blot analysis demonstrated that Igfbp-1 protein was significantly (5 fold) induced by TCDD in wild-type mice (Fig. 3), but not in *Ahr* KO mice, showing 6-fold higher Igfbp-1 protein levels.

Triglycerides concentration measurement

Since an antibody against Lpl is not commercially available, we sought to determine the Lpl activity to evaluate changes in the hepatic Lpl expression level. Lpl is the primary enzyme responsible for the metabolism of triglycerides. We investigated whether the differences in the Lpl expression level in liver might be inversely correlated with the serum triglyceride levels. The serum triglyceride level was lower in *Ahr* KO mice than in wild-type mice, being inversely correlated with the Lpl expression level. However, the serum triglyceride level was significantly (1.3 fold) increased by TCDD treatment in wild-type mice, but not in *Ahr* KO mice (Fig. 4).

DISCUSSION

DNA microarray technology has been extensively used as a powerful tool for predicting unknown signaling pathways. Using DNA microarray analysis, the changes in mRNA expression levels in smooth muscle cells in *Ahr* KO mice were investigated by Guo *et al.* (2004) who found that transforming growth factor-beta 3 (*Tgfb3*) expression was higher in *Ahr* KO mice than in wild-type mice, indicating that Ahr suppresses *Tgfb3* gene expression. It is well known that Ahr regulates various drug-

Table 3. Up- or down-regulated genes in *Ahr* KO mice.

Gene name	Genbank ID	Common name	Relative mRNA expression 7 w	60 w
Up regulation (23 genes)				
Cancer				
Rab38, member of RAS oncogene family	NM_028238	Rab38	2.1	4.3
Vav2 oncogene	NM_009500	Vav2	2.1	2.2
Cell cycle regulator				
Cyclin B2	NM_007630	Ccnb2	3.8	2.1
Enzyme				
Aldo-keto reductase family 1, member B7	NM_009731	Akr1b7	2.0	2.6
Arylacetamide deacetylase (esterase)	NM_023383	Aadac	2.5	2.0
Asparagine synthetase	U38940	Asns	6.5	5.0
Cis-retinol/3alpha hydroxysterol short-chain dehydrogenase-like	BC018263	CRAD-L	3.2	3.1
Cytochrome c oxidase, subunit VIIa 1	NM_009944	Cox7a1	2.8	2.1
Cytochrome P450, family 4, subfamily a, polypeptide 14	NM_007822	Cyp4a14	3.6	4.1
Cytochrome P450, family 17, subfamily a, polypeptide 1	NM_007809	Cyp17a1	12.5	2.1
Glutaredoxin 2 (thioltransferase)	NM_023505	Glrx2	2.3	2.2
Hydroxysteroid (17-beta) dehydrogenase 9	NM_013786	Hsd17b9	3.0	3.5
Lipoprotein lipase	NM_008509	Lpl	14.0	5.5
Methylmalonyl-Coenzyme A mutase	NM_008650	Mut	23.6	9.8
RIKEN cDNA 2310016A09 gene	BC024580	RIKEN	4.7	2.7
Motor				
Dynein, axonemal, intermediate chain 1	AK004387	Dnaic1	4.1	8.2
Signal transducer				
Insulin-like growth factor binding protein 1	NM_008341	Igfbp1	3.2	4.8
Structural protein				
CD59a antigen	NM_007652	Cd59a	8.4	3.7
Collectin sub-family member 11	AK003121	Colec11	2.2	2.3
Olfactory receptor 65 (Olfr65)	NM_013617	Olfr65	2.3	2.5
Transport				
Fatty acid binding protein 5, epidermal	NM_010634	Fabp5	2.3	2.7
Solute carrier organic anion transporter family, member 1a4	NM_030687	Slco1a4	2.9	2.3
Others				
Ubiquitin-associated protein 1	NM_023305	Ubap1	5.8	3.3

Table 3. (Continued)

Gene name	Genbank ID	Common name	Relative mRNA expression 7 w	60 w
Down regulation (20 genes)				
Enzyme				
Betaine-homocysteine methyltransferase	NM_016668	Bhmt	0.48	0.49
Cytochrome P450, family 1, subfamily a, polypeptide 2	NM_009993	Cyp1a2	0.30	0.36
Dopachrome tautomerase	NM_010024	Dct	0.26	0.32
Glutathione peroxidase 6	NM_145451	Gpx6	0.45	0.37
Interferon gamma-induced GTPase	NM_018738	Igtp	0.28	0.27
Isovaleryl coenzyme A dehydrogenase	NM_019826	Ivd	0.16	0.18
NADH dehydrogenase (ubiquinone) Fe-S protein 5	NM_134104	Ndufs5	0.02	0.01
Sulfotransferase family 5A, member 1	NM_020564	Sult5a1	0.30	0.29
UDP glucuronosyltransferase 1 family, polypeptide A6	U16818	Ugt1a6	0.38	0.48
Expressed sequence AI586015	NM_019992	AI586015	0.26	0.42
RIKEN cDNA E430034L04 gene	NM_011816	RIKEN	0.43	0.42
Immunity				
Plasminogen	NM_008877	Plg	0.49	0.40
Signal transducer				
Transforming growth factor beta 1 induced transcript 4	NM_009366	Tgfb1i4	0.23	0.46
Structural protein				
Growth arrest specific 5	NM_013525	Gas5	0.27	0.46
Prion protein	NM_011170	Prnp	0.48	0.50
Transport				
Amiloride-sensitive cation channel 5, intestinal	NM_021370	Accn5	0.12	0.23
Aquaporin 8	NM_007474	Aqp8	0.46	0.39
Solute carrier family 2 (facilitated glucose transporter), member 2	NM_031197	Slc2a2	0.47	0.26
Solute carrier family 22 (organic anion transporter), member 7	NM_144856	Slc22a7	0.35	0.47
Sorting nexin 1	NM_019727	Snx1	0.42	0.45

Up-regulated and down-regulated genes showed more than 200% and less than 50% expressions, respectively, compared with those in wild-type mice at the same weeks old.
Categories of first occurrence in Table 2 are listed.

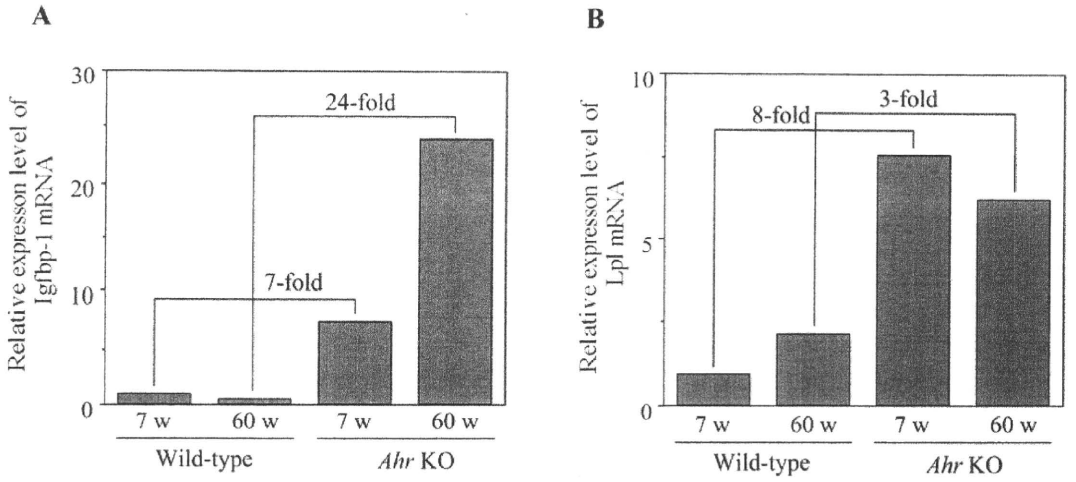

Fig. 1. Relative expression levels of (A) *Igfbp-1* and (B) *Lpl* mRNA in the liver of *Ahr* KO and wild-type mice determined by real-time RT-PCR. Total RNA was extracted from 7- and 60-week-old *Ahr* KO or wild-type mice. Samples from 5 - 7 mice were pooled within each group. The expression levels of *Igfbp-1* and *Lpl* mRNA were normalized with the expression level of GAPDH as a control. Data are expressed as the mean of duplicate experiments.

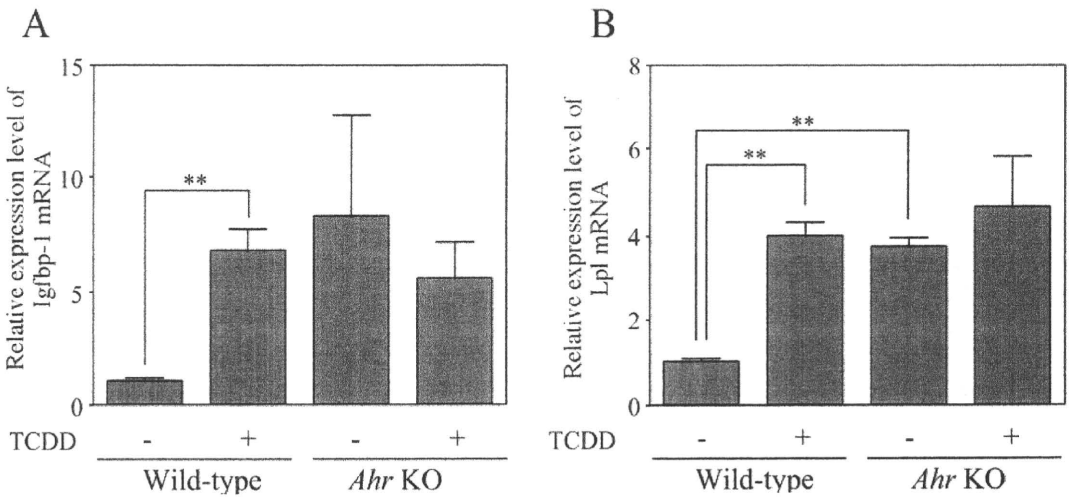

Fig. 2. Effects of TCDD treatment on the expression levels of (A) *Igfbp-1* and (B) *Lpl* mRNA in the liver of *Ahr* KO and wild-type mice determined by real-time RT-PCR analysis. TCDD (40 μg/kg weight) or corn oil was intraperitoneally administered to *Ahr* KO (35-week-old) and wild-type (14-week-old) mice for 4 days. The expression levels of *Igfbp-1* and *Lpl* mRNA were normalized with the expression level of GAPDH as a control. Data are expressed as mean ± S.E. from 5 or 6 mice. $^{**}P < 0.01$ by ANOVA.

metabolizing enzymes in liver. In the present study, we sought to investigate the mRNA profiles in liver from *Ahr* KO mice using microarray to find new Ahr gene targets. The overall gene expression profiles vary during development and the aging process. Therefore, we compared the data in young (7-week-old) and older (60-week-old) mice to determine common changes in gene expression by *Ahr* KO. The decreases in Cyp1a2 and Ugt1a6 in *Ahr* KO mice were consistent with those previously reported (Fernandez-Salguero *et al.*, 1995). In addition, the

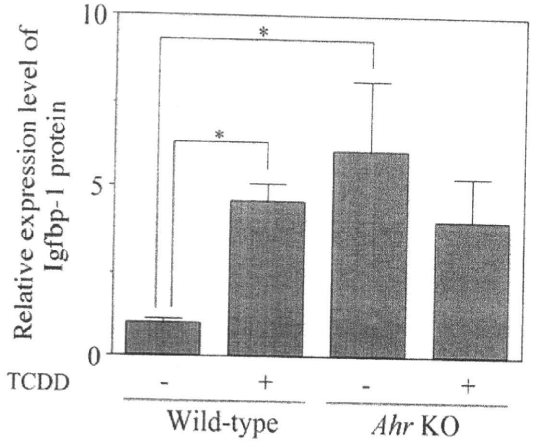

Fig. 3. Effects of TCDD treatment on the expression level of Igfbp-1 protein level in the liver of *Ahr* KO and wild-type mice. TCDD (40 μg/kg weight) or corn oil was intraperitoneally administered to *Ahr* KO (35-week-old) and wild-type (14-week-old) mice for 4 days. Data are expressed as mean ± S.E. from 5 or 6 mice. $*P < 0.05$ by ANOVA.

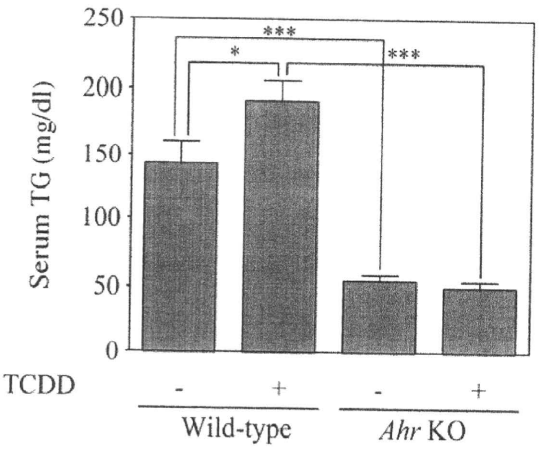

Fig. 4. Effects of TCDD treatment on serum triglyceride level in *Ahr* KO and wild-type mice. TCDD (40 μg/kg weight) or corn oil was administered to *Ahr* KO (35-week-old) and wild-type (14-week-old) mice for 4 days. Data are expressed as mean ± S.E. from 5 or 6 mice. $*P < 0.05$, $***P < 0.001$ by ANOVA.

decrease of Slc22a7 and increase of Cyp17a1 in livers in *Ahr* KO mice were consistent with a recent report by Tijet *et al.* (2006). These results suggest that our study was sufficiently reliable. In the present study, we first found that the *Igfbp-1* and *Lpl* expression levels were higher in *Ahr* KO mice.

Despite the fact that the expression levels of Igfbp-1 and Lpl in the liver were increased in the *Ahr* KO, they were induced by TCDD in an Ahr-dependent manner. The latter results suggested that Ahr positively regulates Igfbp-1 and Lpl in the presence of the ligands. This is supported by a previous report indicating that a xenobiotic responsive element (XRE) to which Ahr binds is located in the promoter region of the *Igfbp-1* gene at -87 (Marchand *et al.*, 2005). In addition, we found two XRE sequences in the promoter region of the *Lpl* gene at -332 and -443 by a computer-assisted homology search. Further study will be necessary to determine whether the binding of Ahr to XRE might be responsible for the induction of Lpl by TCDD. Based on the higher expression levels of Igfbp-1 and Lpl in *Ahr* KO mice compared to those in the wild-type mice, Ahr might suppress Igfbp-1 and Lpl expressions in the absence of exogenous ligands and TCDD may interfere with the suppression. Alternatively, Ahr might positively regulate some suppressor of Igfbp-1 and Lpl expression in the absence of exogenous ligands.

IGFBP-1, one of the six IGFBPs, capable of sequestering insulin growth factors (IGF)s from their receptor. It was reported that transgenic mice of human *IGFBP-1* gene showed postnatal growth retardation and impaired fecundity (Schneider *et al.*, 2000). The pathophysiological abnormalities in *Ahr* KO mice such as decreased body weight, impaired fecundity as well as decrease liver size (Fernandez-Salguero *et al.*, 1995) might be, in part, associated with Igfbp-1 overexpression.

LPL is produced by adipose tissue and then is transported to the endothelial cell surface (Matsumura, 1995). It is also expressed in heart, lung, adipose tissue, kidney, intestine and liver in mice (Kirchgessner *et al.*, 1987). Lpl hydrolyses triglycerides. In *Ahr* KO mice, Lpl expression in adipocytes might also be increased in addition to that in liver, because the serum triglyceride levels in *Ahr* KO mice were decreased. The serum triglyceride level was increased by TCDD treatment in wild-type mice, being consistent with a previous report showing that adipose Lpl activity was decreased by TCDD treatment (Matsumura, 1995). TCDD inhibits the differentiation of preadipocytes to adipocytes (Alexander *et al.*, 1998). The differentiation increases peroxisome proliferator activated receptor (PPAR) γ expression, which is a major regulator of Lpl in adipocytes. Therefore, the increase of serum trigrycerides by TCDD in wild-type mice was, in part, due to the inhibition of adipogenesis.

In summary, we found that hepatic Igfbp-1 and Lpl were paradoxically up-regulated by the activation and

knockout of Ahr. Ahr would be responsible for glucose homeostasis and lipid metabolism.

ACKNOWLEDGEMENT

We thank Mr. Brent Bell for reviewing the manuscript.

REFERENCES

Adachi, J., Mori, Y., Matsui, S. and Matsuda, T. (2004): Comparison of gene expression patterns between 2,3,7,8-tetrachlorodibenzo-*p*-dioxin and a natural arylhydrocarbon receptor ligand, indirubin. Toxicol. Sci., **80**, 161-169.

Alexander, D.L., Ganem, L.G., Fernandez-Salguero, P., Gonzalez, F. and Jefcoate, C.R. (1998): Aryl-hydrocarbon receptor is an inhibitory regulator of lipid synthesis and of commitment to adipogenesis. J. Cell Sci., **111**, 3311-3322.

Andreola, F., Calvisi, D.F., Elizondo, G., Jakowlew, S.B., Mariano, J., Gonzalez, F.J. and De Luca, L.M. (2004): Reversal of liver fibrosis in aryl hydrocarbon receptor null mice by dietary vitamin A depletion. Hepatology, **39**, 157-166.

Andreola, F., Fernandez-Salguero, P.M., Chiantore, M.V., Petkovich, M.P., Gonzalez, F.J. and De Luca, L.M. (1997): Aryl hydrocarbon receptor knockout mice ($AHR^{-/-}$) exhibit liver retinoid accumulation and reduced retinoic acid metabolism. Cancer Res., **57**, 2835-2838.

Bock, K.W. (1994): Aryl hydrocarbon or dioxin receptor: biologic and toxic responses. Rev. Physiol. Biochem. Pharmacol., **125**, 1-42.

Fernandez-Salguero, P., Pineau, T., Hilbert, D.M., McPhail, T., Lee, S.S., Kimura, S., Nebert, D.W., Rudikoff, S., Ward, J.M. and Gonzalez, F.J. (1995): Immune system impairment and hepatic fibrosis in mice lacking the dioxin-binding Ah receptor. Science, **268**, 722-726.

Fernandez-Salguero, P.M., Ward, J.M., Sundberg, J.P. and Gonzalez, F.J. (1997): Lesions of aryl-hydrocarbon receptor-deficient mice. Vet. Pathol., **34**, 605-614.

Guo, J., Sartor, M., Karyala, S., Medvedovic, M., Kann, S., Puga, A., Ryan, P. and Tomlinson, C.R. (2004): Expression of genes in the TGF-β signaling pathway is significantly deregulated in smooth muscle cells from aorta of aryl hydrocarbon receptor knockout mice. Toxicol. Appl. Pharmacol., **194**, 79-89.

Kirchgessner, T.G., Svenson, K.L., Lusis, A.J. and Schotz, M.C. (1987): The sequence of cDNA encoding lipoprotein lipase. A member of a lipase gene family. J. Biol. Chem., **262**, 8463-8466.

Marchand, A., Tomkiewicz, C., Marchandeau, J.-P., Boitier, E., Barouki, R. and Garlatti, M. (2005): 2,3,7,8-Tetrachlorodibenzo-*p*-dioxin induces insulin-like growth factor binding protein-1 gene expression and counteracts the negative effect of insulin. Mol. Pharmacol., **67**, 444-452.

Matsumura, F. (1995): Mechanism of action of dioxin-type chemicals, pesticides, and other xenobiotics affecting nutritional indexes. Am. J. Clin. Nutr., **61**, 695-701.

Mimura, J., Yamashita, K., Nakamura, K., Morita, M., Takagi, T.N., Nakao, K., Ema, M., Sogawa, K., Yasuda, M., Katsuki, M. and Fujii-Kuriyama, Y. (1997): Loss of teratogenic response to 2,3,7,8-tetrachlorodibenzo-*p*-dioxin (TCDD) in mice lacking the Ah (dioxin) receptor. Genes Cells, **2**, 645-654.

Rowlands, J.C. and Gustafsson, J.Å. (1997): Aryl hydrocarbon receptor-mediated signal transduction. Crit. Rev. Toxicol., **27**, 109-134.

Schmidt, J.V. and Bradfield, C.A. (1996): Ah receptor signaling pathways. Annu. Rev. Cell Dev. Biol., **12**, 55-89.

Schmidt, J.V., Su, G.H., Reddy, J.K., Simon, M.C. and Bradfield, C.A. (1996): Characterization of a murine Ahr null allele: involvement of the Ah receptor in hepatic growth and development. PNAS, **93**, 6731-6736.

Schneider, M.R., Lahm, H., Wu, M., Hoeflich, A. and Wolf, E. (2000): Transgenic mouse models for studying the functions of insulin-like growth factor-binding proteins. FASEB J., **14**, 629-640.

Sogawa, K. and Fujii-Kuriyama, Y. (1997): Ah receptor, a novel ligand-activated transcription factor. J. Biochem., **122**, 1075-1079.

Takemoto, K., Nakajima, M., Fujiki, Y., Katoh, M., Gonzalez, F.J. and Yokoi, T. (2004): Role of the aryl hydrocarbon receptor and Cyp1b1 in the antiestrogenic activity of 2,3,7,8-tetrachlorodibenzo-*p*-dioxin. Arch. Toxicol., **78**, 309-315.

Tijet, N., Boutros, P.C., Moffat, I.D., Okey, A.B., Tuomisto, J. and Pohjanvirta, R. (2006): Aryl hydrocarbon receptor regulates distinct dioxin-dependent and dioxin-independent gene batteries. Mol. Pharmacol., **69**, 140-153.

Zaher, H., Fernandez-Salguero, P.M., Letterio, J., Sheikh, M.S., Fornace, A.J. Jr, Roberts, A.B. and Gonzalez, F.J. (1998): The involvement of aryl hydrocarbon receptor in the activation of transforming growth factor-β and apoptosis. Mol. Pharmacol., **54**, 313-321.

0090-9556/08/3608-1461–1464$20.00
DRUG METABOLISM AND DISPOSITION

DMD 36:1461–1464, 2008

Vol. 36, No. 8
21428/3364142
Printed in U.S.A.

DMD
DRUG METABOLISM AND DISPOSITION
aspet

Short Communication

Expression of UGT1A and UGT2B mRNA in Human Normal Tissues and Various Cell Lines[S]

Received March 11, 2008; accepted May 13, 2008

ABSTRACT:

UDP-glucuronosyltransferases (UGTs) are major phase II drug metabolism enzymes that catalyze the glucuronidation of numerous endogenous and exogenous compounds. UGTs are divided into two families, UGT1 and UGT2, based on evolutionary divergence and homology. Nine UGT1A and seven UGT2B functional isoforms have been identified in humans. Glucuronidation occurs mainly in liver but also in various extrahepatic tissues, possibly affecting the pharmacokinetics. In the present study, we comprehensively determined the expression of all functional UGT1A and UGT2B isoforms in normal human tissues including liver, lung, stomach, small intestine, colon, kidney, bladder, adrenal gland, breast, ovary, uterus, and testis by semiquantitative reverse transcription-polymerase chain reaction. In addition, the expressions of these UGTs mRNA in 15 kinds of human tissue-derived cell lines were also analyzed. Many UGT isoforms were abundantly expressed in the liver, gastrointestinal tract, and kidney, supporting previous studies. Interestingly, we found that all UGTs except UGT2B17 were expressed in bladder. In steroid-related tissues, UGTs were expressed in tissue- and isoform-specific manners. Expression profiles in human tissue-derived cell lines were not necessarily consistent with those in corresponding normal tissues. Different expression profiles were observed in distinct cell lines derived from the same organ. The information presented here will be helpful for understanding the glucuronidation in various tissues and for choosing appropriate cell lines for in vitro studies.

UDP-glucuronosyltransferases (UGTs) are major phase II drug metabolism enzymes in humans (Tukey and Strassburg, 2000). UGTs catalyze the glucuronidation of numerous endogenous compounds such as bilirubin, bile acids, thyroid hormone, and steroid hormones as well as substantial exogenous substrates including therapeutic drugs, carcinogens, and environmental pollutants. Currently, 19 UGT proteins have been identified in humans, and they are divided into three subfamilies, UGT1A, UGT2A, and UGT2B, based on evolutionary divergence and homology (Mackenzie et al., 2005). The human *UGT1A* gene cluster located on chromosome 2q37 contains multiple unique first exons for each UGT1A and common exons 2 to 5 (Ritter et al., 1992), encoding nine kinds of the functional UGT1A subfamily. The *UGT2A* and *UGT2B* genes are located on chromosome 4q13, encoding three and seven functional proteins, respectively. The *UGT2A1* and *UGT2A2* are formed by differential splicing of variable first exons and common exons 2 to 6, likely the *UGT1A* gene. Meanwhile, UGT2A3 and each UGT2B are encoded by individual genes. Until now, the clinical significance of UGT2A protein remains to be clarified. In contrast, it is well known that UGT1A and UGT2B play important roles in the glucuronidation of a variety of endogenous and exogenous compounds.

The liver plays a central role in metabolism, including glucuronidation. Additionally, extrahepatic tissues such as the gastrointestinal tract and kidney also have a role in metabolism (Soars et al., 2002). The distribution of UGT expression in human tissues has been studied mainly in the liver and gastrointestinal tract (Strassburg et al., 2000; Tukey and Strassburg, 2000). In contrast, the expression in other extrahepatic tissues has not been fully studied.

Human tissue-derived cell lines are used as a tool for in vitro drug metabolism studies or induction studies. Hepatoma HepG2 cells and adenocarcinoma Caco-2 cells are frequently used, and the expression of selected UGT isoforms in these cell lines has been reported. However, no study determined the expression of all UGT isoforms in the cell lines. Furthermore, information concerning UGT expression in other cell lines is limited. In the present study, we comprehensively determined the expression of all human UGT isoforms in various normal tissues and human tissue-derived cell lines.

Materials and Methods

Cell Lines and Culture Condition. HepG2 (hepatocellular carcinoma), Caco-2 (colorectal adenocarcinoma), LS180 (colorectal adenocarcinoma), HEK293 (embryonic kidney), ACHN (renal cell adenocarcinoma), HK-2 (renal proximal tubule cell), SW13 (adrenocortical adenocarcinoma), H295R (adrenocortical adenocarcinoma), MDA-MB-435 (breast ductal carcinoma), and MCF-7 (breast epithelial adenocarcinoma) cells were obtained from American Type Culture Collection (Manassas, VA). HuH7 (hepatocellular carcinoma), HeLa (adenocarcinoma of the cervix of uterus), and OMC-3 (ovarian mucinous cystadenocarcinoma) cells were obtained from RIKEN BioResource Center (Ibaraki, Japan). HLE cells (hepatocellular carcinoma) were obtained from the Japan Collection of Research Biosources (Tokyo, Japan). Ishikawa (endometrial adenocarcinoma) cells were generous gifts from Dr. Masato Nishida, Tsukuba University (Ibaraki, Japan).

HLE, HuH7, SW13, MDA-MB-435, HeLa, and Ishikawa cells were cultured in DMEM (Nissui Pharmaceutical, Tokyo, Japan) supplemented with 10% fetal bovine serum (FBS) (Invitrogen, Carlsbad, CA). HepG2, Caco-2, LS180, ACHN, and MCF-7 cells were cultured in DMEM supplemented with

Article, publication date, and citation information can be found at http://dmd.aspetjournals.org.
doi:10.1124/dmd.108.021428.
[S] The online version of this article (available at http://dmd.aspetjournals.org) contains supplemental material.

ABBREVIATIONS: UGT, UDP-glucuronosyltransferase; DMEM, Dulbecco's modified Eagle's medium; FBS, fetal bovine serum; GAPDH, glyceraldehyde-3-phosphate dehydrogenase; RT-PCR, reverse transcriptase-polymerase chain reaction.

TABLE 1

Sequences of primers and annealing temperatures used for RT-PCR analyses

Target	Primer	Sequence	Position[a]	Annealing Temperature
				°C
UGT1A1	1A1-S	5′-CCT TGC CTC AGA ATT CCT TC-3′	696-715	58
	1A-AS	5′-ATT GAT CCC AAA GAG AAA ACC AC-3′	907-929	
UGT1A3	1A3-S	5′-TGT TGA ACA ATA TGT CTT TGG TCT-3′	347-370	58
	1A-AS	5′-ATT GAT CCC AAA GAG AAA ACC AC-3′	910-932	
UGT1A4	1A4-S[b]	5′-ACG CTG GGC TAC ACT CAA GG-3′	277-296	58
	1A4-AS	5′-TCT GAA TTG GTC GTT AGT AAC T-3′	587-608	
UGT1A5	1A5-S	5′-ACA ATA TGT CTT TGA TCA TA-3′	353-372	58
	1A5-AS	5′-AGA AAC AGC ATG GCA AAG-3′	667-684	
UGT1A6	1A6-S	5′-AGA GAA TTT CTG CAG GGG TTT T-3′	26-47	56
	1A6-AS	5′-TTG GAT TCT TTC AAA AGC-3′	195-212	
UGT1A7	1A7-S[c]	5′-TGG CTC GTG CAG GGT GGA CTG-3′	2-22	58
	1A7-AS[c]	5′-TTC GCA ATG GTG CCG TCC AGC-3′	290-310	
UGT1A8	1A8-S	5′-GGT CTT CGC CAG GGG AAT AG-3′	498-517	58
	1A-AS	5′-ATT GAT CCC AAA GAG AAA ACC AC-3′	898-920	
UGT1A9	1A9-S	5′-GAA CAT TTA TTA TGC CAC CG-3′	646-665	58
	1A-AS	5′-ATT GAT CCC AAA GAG AAA ACC AC-3′	898-920	
UGT1A10	1A10-S	5′-CTC TTT CCT ATG TCC CCA ATG A-3′	557-578	58
	1A-AS	5′-ATT GAT CCC AAA GAG AAA ACC AC-3′	898-920	
UGT2B4	2B4-S	5′-CAT CTT CAG CTT CCA TTT C-3′	170-188	52
	2B4-AS	5′-TCC TTA CAG AAC TTT CTA AG-3′	367-386	
UGT2B7	2B7-S[b]	5′-AGT TGG AGA ATT TCA TCA TGC AAC AGA-3′	254-280	58
	2B-AS-1[b]	5′-TCA GCC AGC AGC TCA CCA CAG GG-3′	463-485	
UGT2B10	2B10-S[b]	5′-TGA CAT CGT TTT TGC AGA TGC TTA-3′	432-455	62
	2B-AS-2[b]	5′-CAG GTA CAT AGG AAG GAG GGA A-3′	562-583	
UGT2B11	2B11-S	5′-CTT CCA TTC TTT TTG ATC CCA ATG AT-3′	179-204	58
	2B11-AS	5′-GGA GAC TGT ACA CAA ACC-3′	500-517	
UGT2B15	2B15-S[b]	5′-GTG TTG GGA ATA TTA TGA CTA CAG TAA C-3′	348-375	62
	2B-AS-1[b]	5′-TCA GCC AGC AGC TCA CCA CAG GG-3′	466-488	
UGT2B17	2B17-S[b]	5′-GTG TTG GGA ATA TTC TGA CTA TAA TAT A-3′	348-375	58
	2B-AS-2[b]	5′-CAG GTA CAT AGG AAG GAG GGA A-3′	568-589	
UGT2B28	2B28-S[b]	5′-ATC CCA ATG ACG CAT TCA CTC TTA AAC TC-3′	194-222	62
	2B-AS-2[b]	5′-CAG GTA CAT AGG AAG GAG GGA A-3′	565-586	
GAPDH	hGAPDH-S[d]	5′-CCA GGG CTG CTT TTA ACT C-3′	56-74	52
	hGAPDH-AS[d]	5′-GCT CCC CCC TGC AAA TGA-3′	330-347	

[a] Nucleotide position on cDNA when the A in the initiation codon is 1.
[b] Congiu et al. (2002).
[c] Gardner-Stephen et al. (2004).
[d] Tsuchiya et al. (2004).

10% FBS (Invitrogen) and 0.1 mM nonessential amino acids (Invitrogen). HEK293 cells were cultured in DMEM supplemented with 4.5 g/liter glucose, 10 mM HEPES, and 10% FBS (Invitrogen). OMC-3 cells were cultured in Ham's F12 medium with 10% FBS (BioWhittaker, Walkersville, MD). HK-2 and H295R cells were cultured in DMEM/Ham's F12 supplemented with 10% FBS (Invitrogen), 6.7 μg/liter sodium selenite, 10 mg/liter insulin, and 5.5 mg/liter transferring (ITS-G) (Invitrogen). These cells were maintained at 37°C under an atmosphere of 5% CO_2/95% air.

Total RNA from Normal Human Tissues and Cell Lines. Total RNA samples from human normal tissues were purchased from Stratagene (La Jolla, CA) (liver, colon, kidney, bladder, breast, ovary, and uterus), Clontech (Palo Alto, CA) (stomach, small intestine, adrenal gland, and testis), and Cell Applications (San Diego, CA) (lung). The liver sample was from a single donor, a 45-year-old male. The breast sample was pooled tissues from two female donors, a 39- and a 49-year-old. The colon sample was pooled tissues from two female donors, a 62- and a 67-year-old. The kidney (a 56-year-old male), lung (a 40-year-old male), ovary (a 73-year-old female), and stomach (a 50-year-old male) samples were from single donors. The bladder sample was pooled tissues from two female donors, a 24- and a 42-year-old. The uterus sample was pooled tissues from three female donors, a 54-, a 68-, and a 76-year-old. The testis sample was pooled tissues from 45 whites, ages 19 to 64. The small intestine sample was pooled tissues from 5 male/female whites, ages 20 to 61. The adrenal gland sample was pooled tissues from 62 male/female whites, ages 15 to 61. Information concerning smoking or medication of the donors was not available. Total RNA from each cell line was extracted using ISOGEN (Invitrogen).

RT-PCR Analyses. The cDNA was synthesized from total RNA using ReverTra Ace (TOYOBO, Osaka, Japan) according to the manufacturer's protocol. A 1-μl portion of the reverse-transcribed mixture was added to PCR mixtures (25 μl) consisting of 1× PCR buffer [67 mM Tris-HCl buffer (pH 8.8), 16.6 mM $(NH_4)_2SO_4$, 0.45% Triton X-100, 0.02% gelatin], 1.5 mM $MgCl_2$, 0.4 μM primers, 250 μM dNTPs, and 1 U of Taq DNA polymerase (Greiner Japan, Tokyo, Japan). After an initial denaturation at 94°C for 3 min, the amplification was performed by denaturation at 94°C for 30 s, annealing at an appropriate temperature for 30 s, and extension at 72°C for 30 s for 35 cycles. The final extension step was performed at 72°C for 5 min. The sequences of primers used in the present study and the annealing temperatures are shown in Table 1. The PCR products (15 μl) were analyzed by electrophoresis with 2% agarose gel and visualized by ethidium bromide staining. The specificity of all primer pairs (Supplemental Fig. 1) was confirmed by digestion of the PCR products with appropriate restriction enzymes. Expression of GAPDH mRNA was used as an internal control for the cDNA quantity and quality.

Results

UGT mRNA Expression in Human Normal Tissues. RT-PCR analyses were performed to determine the mRNA expression of the UGT isoforms in human normal tissues (Fig. 1). UGT1A1 was highly expressed in liver, gastrointestinal tract, and bladder. UGT1A3 was expressed in a similar pattern to that of UGT1A1. Expression of UGT1A4 was widely observed in all tissues except breast. It was highest in liver and moderate in gastrointestinal tract, kidney, bladder, and ovary. UGT1A5 was expressed in gastrointestinal tract, kidney, bladder, and uterus and was marginally detected in the other tissues. UGT1A6 was expressed in liver, gastrointestinal tract, kidney, and bladder. UGT1A7 and UGT1A8 were detected in small intestine, colon, kidney, and bladder. UGT1A9 was highly expressed in liver and kidney and marginally in

DMD DRUG METABOLISM AND DISPOSITION aspet

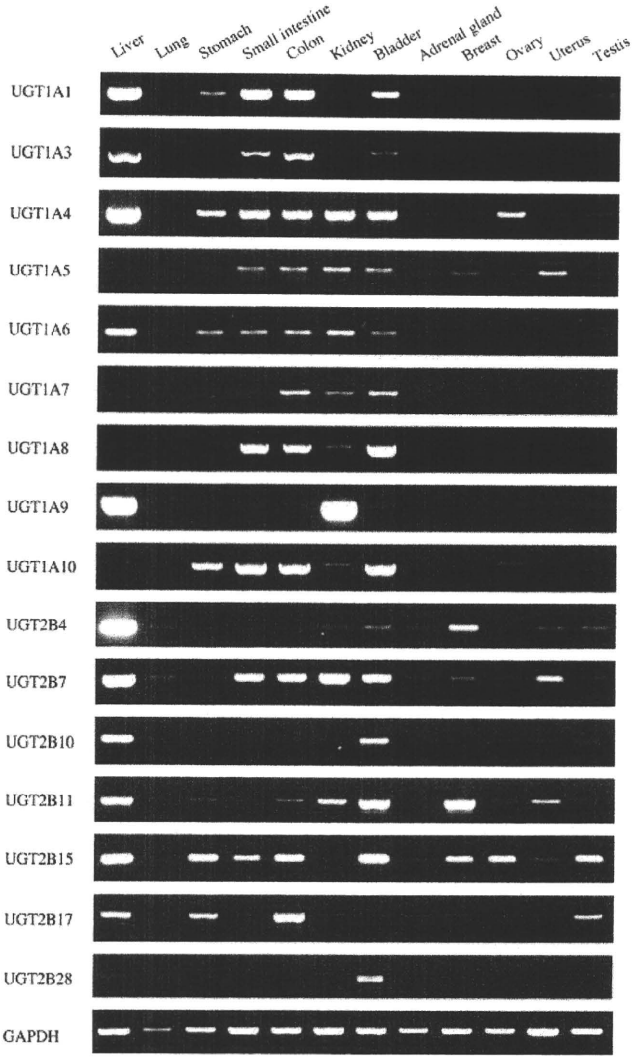

FIG. 1. RT-PCR analyses of UGT mRNA in human normal tissues. Total RNA samples from human normal tissues were analyzed by RT-PCR using primers specific for each UGT isoform.

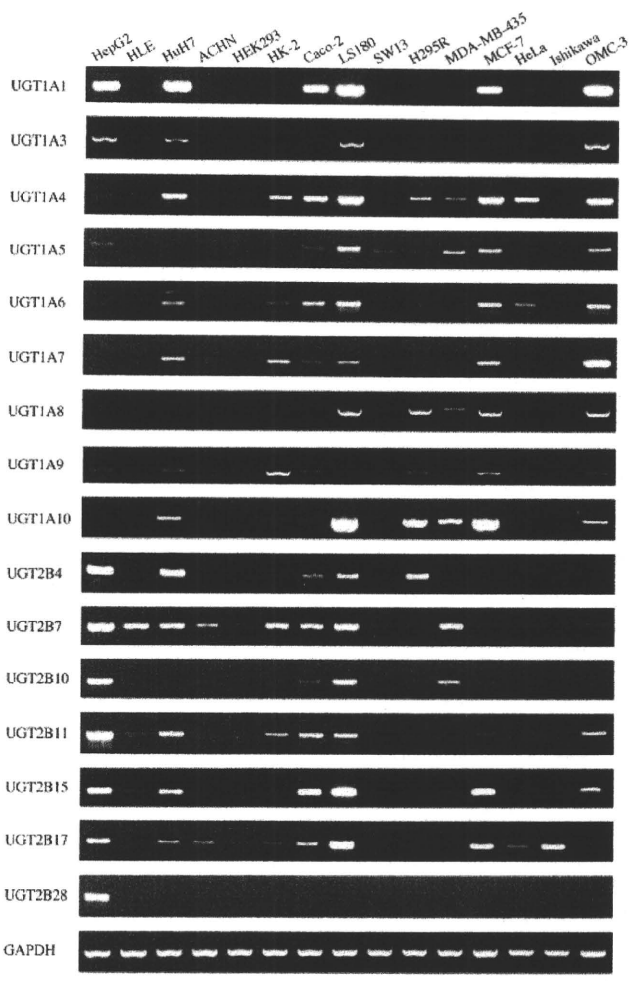

FIG. 2. RT-PCR analyses of UGT mRNA in human tissue-derived cell lines. Total RNA samples from various cell lines were analyzed by RT-PCR using primers specific for each UGT isoform.

small intestine, colon, bladder, and testis. UGT1A10 was mainly expressed in gastrointestinal tract and bladder and marginally expressed in liver, kidney, ovary, and uterus. UGT2B4 was highly expressed in liver, moderately in breast, and marginally in the other tissues. UGT2B7 was expressed in all tissues, highly in liver, small intestine, colon, kidney, bladder, and uterus. UGT2B10 was highly expressed in liver and bladder. UGT2B11 was highly expressed in liver, bladder, and breast and moderately in kidney and uterus. UGT2B15 was highly expressed in liver, gastrointestinal tract, bladder, breast, ovary, and testis. UGT2B17 was highly expressed in liver, stomach, colon, and testis. UGT2B28 was highly expressed in bladder and marginally in liver, stomach, and breast.

UGT mRNA Expression in Human Tissue-Derived Cell Lines. The expression of UGT mRNA in various human tissue-derived cell lines is shown in Fig. 2. UGT1A1 was highly expressed in HepG2, HuH7, Caco-2, LS180, MCF-7, and OMC-3 cells and marginally in HK-2, H295R, MDA-MB-435, and HeLa cells. UGT1A3 was detected in HepG2, HLE, HuH7, Caco-2, LS180, MCF-7, and OMC-3 cells. The expression profile of UGT1A4 was similar to that of UGT1A1. UGT1A5 was highly expressed in LS180, MDA-MB-435, MCF-7, and OMC-3 cells. UGT1A6 was detected in HepG2, HuH7, HK-2, Caco-2, LS180, H295R, MCF-7, HeLa, Ishikawa, and OMC-3 cells. The expression profiles of UGT1A7 and UGT1A9 were nearly identical to that of UGT1A6. UGT1A8 was highly expressed in LS180, H295R, MDA-MB-435, MCF-7, and OMC-3 cells. UGT1A10 was highly expressed in LS180 and MCF-7 cells, followed by H295R, MDA-MB-435, HuH7, and OMC-3 cells. UGT2B4 was highly expressed in HepG2 and HuH7, followed by H295R, LS180, Caco-2, and HK-2 cells. UGT2B7 was expressed in all cell lines. UGT2B10 was highly expressed in HepG2, LS180, and MDA-MB-435 cells. UGT2B11 was highly expressed in HepG2, HuH7, HK-2, Caco-2, LS180, and OMC-3 cells. UGT2B15 was highly expressed in HepG2, HuH7, Caco-2, LS180, MCF-7, and OMC-3 cells. The UGT2B17 mRNA was highly expressed in HepG2, LS180, MCF-7, and Ishikawa cells. UGT2B28 was expressed only in HepG2 cells.

Discussion

We determined the expression levels of the functional UGT1A and UGT2B isoforms in human normal tissues and human tissue-derived cell lines. Because of the limited availability of antibodies that are specific for each UGT isoform as well as overlapping substrate specificities, it was difficult to evaluate the protein level. In contrast, the mRNA levels for each isoform can be specifically determined by RT-PCR using specific primers. For this reason, we determined the UGT mRNA levels.

The expression profiles of the UGT1A and UGT2B isoforms in liver, gastrointestinal tract, and kidney were largely consistent with those of previous studies (King et al., 2000; Tukey and Strassburg, 2000). The UGTs in these tissues would contribute to the first-pass effects and clearance of drugs, as a previous study (Soars et al., 2002) demonstrated that the microsomes from these tissues had certain abilities of glucuronidation. In disagreement with previous studies (Ritter et al., 1992; Tukey and Strassburg, 2000), the present study detected the expression of UGT1A1 in kidney and UGT1A10 in liver, although the levels were extremely low (Fig. 1). This discrepancy may be due to interindividual differences in the UGT expression. Additionally, differences in the experimental conditions in PCR and/or the primers between the present and previous studies may also have affected the results.

This is the first study to determine comprehensively the mRNA expression of each UGT isoform in human lung, bladder, and steroid-related tissues. The UGTs were hardly expressed in lung in this study. Meanwhile, all UGT1A and UGT2B isoforms except UGT2B17 were expressed in bladder. Giuliani et al. (2005) have reported that UGT1A protein was detected in normal bladder by immunohistochemistry. Since the bladder is exposed to numerous xenobiotics, UGTs expressed in bladder would also contribute to the detoxification of xenobiotics, possibly participating in the protection from toxins. Our finding of the substantial expression of UGTs in bladder may provoke researchers to investigate the glucuronidation capabilities of bladder microsomes. We found that the UGTs were also expressed in steroid-related tissues in isoform-specific manners. However, the present study unfortunately could not determine the interindividual variability of the expression levels of UGTs, because the RNA samples we used were from an individual sample or pooled samples. Strassburg et al. (2000) reported that the UGT1A and UGT2B isoforms were present in gastrointestinal tissues from some individuals but were absent in those from other individuals. The interindividual differences in the expression may partly result from genetic polymorphisms, because genetic polymorphisms on the promoter or coding region affect the transcriptional activity or mRNA stability. Actually, in the *UGT2B17* gene, a deletion allele has been reported (Wilson et al., 2004). Although we did not determine the genotype of *UGT2B17* in our samples, polymorphisms may affect the variability of UGT2B17 expression. In addition to genetic polymorphisms, the induction by environmental and/or dietary factors or differences in the levels of transcriptional factors would be causal factors of the variability of the UGT expression. It would be worth elucidating the interindividual variability in UGT expression in steroid-related tissues and bladder. Finally, previous immunohistochemical studies demonstrated that UGTs localize in certain cell type or specific region in tissues such as small intestine (Strassburg et al., 2000), kidney (Gaganis et al., 2007), bladder (Giuliani et al., 2005), breast (Gestl et al., 2002), and uterus (Lépine et al., 2004). However, the studies with total RNA from whole tissue cannot specify the expression in a specific cell type. We should keep this point in mind to predict or extrapolate the role of the expressed UGTs on metabolism of drugs, carcinogens, and endogenous compounds.

The expression profiles of UGT mRNA in the human tissue-derived cell lines were not necessarily consistent with those in corresponding normal tissues. HLE cells showed no detectable UGT1A expression, albeit they are derived from liver. Although the reasons remain unclear, HLE cells would not be suitable for the study of UGT1A expression. In LS180 cells that are derived from colon, all UGT1A and UGT2B isoforms except for UGT2B28 were expressed. This cell line might be an appropriate tool for in vitro studies of the expression and regulation of UGTs. It was interesting that MCF-7 cells, which are estrogen receptor-positive (Guthrie et al., 1997) breast epithelial adenocarcinoma cells, expressed all UGT1A isoforms, but MDA-MB-435 cells, which are estrogen receptor-negative (Guthrie et al., 1997) breast ductal carcinoma cells, expressed limited kinds of UGT1A isoforms. It was also interesting that the expression levels of UGT2B7 and UGT2B10 were higher in MDA-MB-435 cells than in MCF-7 cells, but those of UGT2B15 and UGT2B17 were higher in MCF-7 cells than in MDA-MB-435 cells. Collectively, the expression profiles of UGT mRNA in the cell lines show diversity, although the derived organs were the same. The information presented here would be useful for choosing suitable cell lines for in vitro studies on UGTs.

In summary, we comprehensively determined the expression profiles of UGT1A and UGT2B in human normal tissues and human tissue-derived cell lines. The findings will be useful for understanding the physiological significance of each UGT isoform and to predict the capabilities of glucuronidation in various tissues. In addition, our results provide basic information on UGT expression in various kinds of cell lines.

Acknowledgments. We acknowledge Brent Bell for reviewing the manuscript.

Drug Metabolism and Toxicology, Division of Pharmaceutical Sciences, Graduate School of Medical Science, Kanazawa University, Kanazawa, Japan

Akiko Nakamura
Miki Nakajima
Hiroyuki Yamanaka
Ryoichi Fujiwara
Tsuyoshi Yokoi

References

Congiu M, Mashford ML, Slavin JL, and Desmond PV (2002) UDP glucuronosyltranferase mRNA levels in human liver disease. *Drug Metab Dispos* **30:**129–134.

Gaganis P, Miners JO, Brennan JS, Thomas A, and Knights KM (2007) Human renal cortical and medullary UDP-glucuronosyltransferases (UGTs): immunohistochemical localization of UGT2B7 and UGT1A enzymes and kinetic characterization of *S*-naproxen glucuronidation. *J Pharmacol Exp Ther* **323:**422–430.

Gardner-Stephen D, Heydel JM, Goyal A, Lu Y, Xie W, Lindblom T, Mackenzie P, and Radominska-Pandya A (2004) Human PXR variants and their differential effects on the regulation of human UDP-glucuronosyltransferase gene expression. *Drug Metab Dispos* **32:**340–347.

Gestl SA, Green MD, Shearer DA, Frauenhoffer E, Tephly TR, and Weisz J (2002) Expression of UGT2B7, a UDP-glucuronosyltransferase implicated in the metabolism of 4-hydroxyestrone and all-*trans* retinoic acid, in normal human breast parenchyma and in invasive and *in situ* breast cancers. *Am J Pathol* **160:**1467–1479.

Giuliani L, Ciotti M, Stoppacciaro A, Pasquini A, Silvestri I, De Matteis A, Frati L, and Agliano AM (2005) UDP-glucuronosyltransferases 1A expression in human urinary bladder and colon cancer by immunohistochemistry. *Oncol Rep* **13:**185–191.

Guthrie N, Gapor A, Chambers AF, and Carroll KK (1997) Inhibition of proliferation of estrogen receptor-negative MDA-MB-435 and -positive MCF-7 human breast cancer cells by palm oil tocotrienols and tamoxifen, alone and in combination. *J Nutr* **127:**544S–548S.

King CD, Rios GR, Green MD, and Tephly TR (2000) UDP-glucuronosyltransferases. *Curr Drug Metab* **1:**143–161.

Lépine J, Bernard O, Plante M, Têtu B, Pelletier G, Labrie F, Bélanger A, and Guillemette C (2004) Specificity and regioselectivity of the conjugation of estradiol, estrone, and their catecholestrogen and methoxyestrogen metabolites by human uridine diphosphoglucuronosyltransferases expressed in endometrium. *J Clin Endocrinol Metab* **89:**5222–5232.

Mackenzie PI, Bock KW, Burchell B, Guillemette C, Ikushiro S, Iyanagi T, Miners JO, Owens IS, and Nebert DW (2005) Nomenclature update for the mammalian UDP glycosyltransferase (*UGT*) gene superfamily. *Pharmacogenet Genomics* **15:**677–685.

Ritter JK, Chen F, Sheen YY, Tran HM, Kimura S, Yeatman MT, and Owens IS (1992) A novel complex locus *UGT1* encodes human bilirubin, phenol, and other UDP-glucuronosyltransferase isozymes with identical carboxyl termini. *J Biol Chem* **267:**3257–3261.

Soars MG, Burchell B, and Riley RJ (2002) In vitro analysis of human drug glucuronidation and prediction of in vivo metabolic clearance. *J Pharmacol Exp Ther* **301:**382–390.

Strassburg CP, Kneip S, Topp J, Obermayer-Straub P, Barut A, Tukey RH, and Manns MP (2000) Polymorphic gene regulation and interindividual variation of UDP-glucuronosyltransferase activity in human small intestine. *J Biol Chem* **275:**36164–36171.

Tsuchiya Y, Nakajima M, Kyo S, Kanaya T, Inoue M, and Yokoi T (2004) Human CYP1B1 is regulated by estradiol via estrogen receptor. *Cancer Res* **64:**3119–3125.

Tukey RH and Strassburg CP (2000) Human UDP-glucuronosyltransferases: metabolism, expression, and disease. *Annu Rev Pharmacol Toxicol* **40:**581–616.

Wilson W III, Pardo-Manuel de Villena F, Lyn-Cook BD, Chatterjee PK, Bell TA, Detwiler DA, Gilmore RC, Valladeras IC, Wright CC, Threadgill DW, et al. (2004) Characterization of a common deletion polymorphism of the *UGT2B17* gene linked to *UGT2B15*. *Genomics* **84:**707–714.

Address correspondence to: Dr. Miki Nakajima, Drug Metabolism and Toxicology, Division of Pharmaceutical Sciences, Graduate School of Medical Science, Kanazawa University, Kakuma-machi, Kanazawa 920-1192, Japan. E-mail: nmiki@kenroku.kanazawa-u.ac.jp

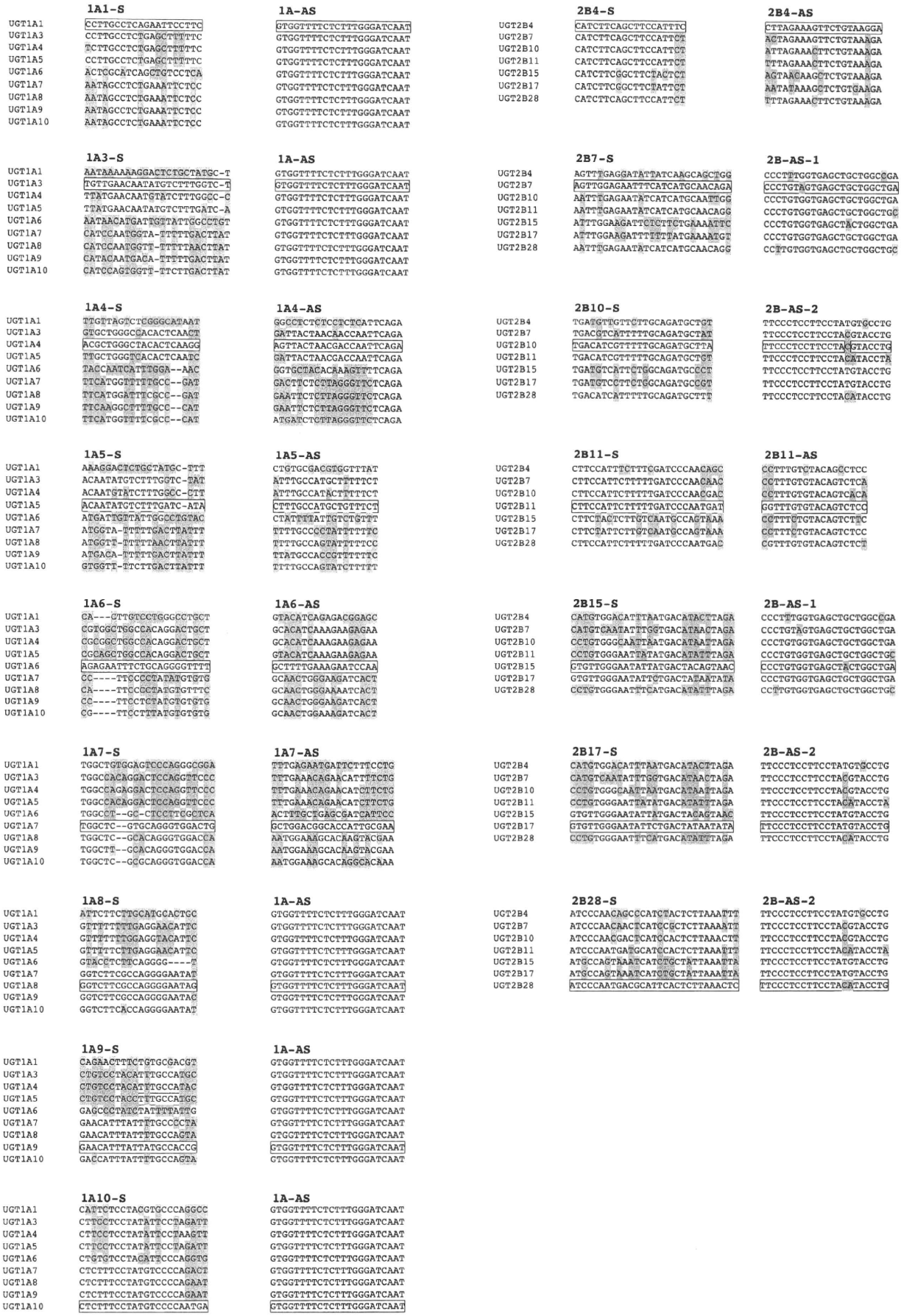

Supplemental Fig. 1. The specificity of primers used in this study. Multiple sequence alignments were generated using ClustalW (http://clustalw.ddbj.nig.ac.jp/top-j.html). The names of primers are shown in bold letters. The sequences to which the concerned primer anneal are boxed. Mismatched sequences with primer are shaded.

0090-9556/08/3609-1745–1752$20.00
DRUG METABOLISM AND DISPOSITION

DMD 36:1745–1752, 2008

Vol. 36, No. 9
21469/3367834
Printed in U.S.A.

Species Differences in UDP-Glucuronosyltransferase Activities in Mice and Rats

Hirotada Shiratani, Miki Katoh, Miki Nakajima, and Tsuyoshi Yokoi

Drug Metabolism and Toxicology, Division of Pharmaceutical Sciences, Graduate School of Medical Science, Kanazawa University, Kanazawa, Japan

Received March 17, 2008; accepted May 22, 2008

ABSTRACT:

UDP-glucuronosyltransferases (UGTs), expressed in various tissues including liver and intestine, catalyze phase II metabolic biotransformation. There is little information on species differences between mice and rats in UGT activities, especially in intestine. The purpose of the present study was to clarify the species differences between mice and rats in UGT activities using duodenal and liver microsomes. For estradiol 3-*O*-glucuronidation in duodenal microsomes, the kinetic data in mice were fit to the Hill equation. However, the Hill coefficient was low in rats (n = 1.1), suggesting that rat estradiol 3-*O*-glucuronidation followed the Michaelis-Menten equation rather than the Hill equation. For 4-nitrophenol (4-NP) *O*-glucuronidation, the K_m values were different between mice and rats. The intrinsic clearance (CL_{int}) values for mycophenolic acid (MPA) *O*- and morphine 3-*O*-glucuronidation in male mouse duodenum were 3- and 17-fold lower than those in rat, respectively. In male liver, the CL_{int} values for 4-NP *O*-, propofol *O*-, MPA *O*-, and morphine 3-*O*-glucuronidation and the CL_{max} value for 4-methylumbelliferone *O*-glucuronidation in mice were higher than those in rats. The CL_{max} value for estradiol 3-*O*-glucuronidation in mice was lower than that in rats. Also, there were strain differences among C57BL/6J, BALB/c, C3H/HeJ, DBA/2, ddY, and ICR mice in UGT activities in duodenum. We clarified that the species differences in UGT activity evaluated by the CL_{int} or CL_{max} values in liver and duodenum varied according to the substrate.

UDP-glucuronosyltransferase (UGT) expressed in various tissues including liver and intestine catalyzes phase II metabolic biotransformation. UGTs conjugate lipophilic compounds with glucuronic acid from UDP-glucuronic acid (UDPGA), thereby increasing hydrophilicity and enhancing excretion through bile and urine (Dutton, 1980). In both humans and rodents, two families of UGT, UGT1 and UGT2, are known. The human *UGT1* gene contains 13 individual promoter/first exons and shares exons 2 to 5 (Mackenzie et al., 2005). As with the human genes, rat and mouse *Ugt1* genes also share exons 2 to 5 and have 10 and 14 first exons, respectively (Mackenzie et al., 2005). Among species, the numbers of the first exons and pseudogenes differ. There are four, two, and five pseudogenes in human, rat, and mouse UGT enzymes, respectively. For example, human *UGT1A4* is functional but rat *UGT1A4* and mouse *Ugt1a4* are pseudogenes. Human *UGT1A9* and mouse *Ugt1a9* are functional, but rat *UGT1A9* is a pseudogene. In the case of *UGT1A6*, mice have two functional copies of *Ugt1a6*, *Ugt1a6a* and *Ugt1a6b*, whereas humans and rats have one copy of *UGT1A6*. On the other hand, the *UGT2* gene in humans, rats, and mice consists of six exons, except for *UGT2A1* and *UGT2A2* genes (seven exons). The UGT2 family contains three enzymes of the UGT2A subfamily and seven enzymes of the UGT2B subfamily among humans, rats, and mice. The UGT2 subfamily shares more than 70% sequence homology, thus orthologs across species are hard to elucidate (Mackenzie et al., 2005). These species differences in UGT genes could result in species differences in UGT activities.

Liver and intestine are the important tissues for drug metabolism including glucuronidation. The expression of UGT mRNAs has been reported in various tissues in humans (Tukey and Strassburg, 2000), rats (Shelby et al., 2003), and mice (Buckley and Klaassen, 2007). Comparison of expression levels among UGT enzymes is difficult. Because UGT antibodies are not available for the specific quantification of each UGT enzyme, the expression ratio of each UGT enzyme remains unclear in the liver and intestine. Which UGT enzyme in mice and rats corresponds to human UGT enzyme is controversial.

The UGT substrates include many endogenous and xenobiotic compounds. Typical endogenous substrates are bilirubin and estradiol. In particular, hyperbilirubinemia caused by a *UGT* defect is well known (Burchell et al., 2000). Small xenobiotic planar phenols such as 4-methylumbelliferone (4-MU) and 4-nitrophenol (4-NP) are often used for measuring the glucuronidation (Hanioka et al., 2006). Propofol, widely used as an intravenous anesthetic for the induction and maintenance of anesthesia, is metabolized mainly to its glucuronide in humans (Sneyd et al., 1994). A prodrug of mycophenolic acid (MPA), mycophenolate mofetil (MMF), exhibited severe gastrointestinal toxicity and a relationship between its toxicity and MPA glucuronidation is suspected in rats (Stern et al., 2007). Morphine, an analgesic drug used for the treatment of acute and chronic pain syndromes in cancer patients, is glucuronidated mainly by UGT2B7 in a stereoselective manner to morphine 3-*O*- and 6-*O*-glucuronide in humans (Coffman et al., 1998), whereas the main metabolite in humans and rodents is

H.S. and M.K. contributed equally to this work.

Article, publication date, and citation information can be found at http://dmd.aspetjournals.org.

doi:10.1124/dmd.108.021469.

ABBREVIATIONS: UGT/Ugt, UDP-glucuronosyltransferase; UDPGA, UDP-glucuronic acid; 4-MU, 4-methylumbelliferone; 4-NP, 4-nitrophenol; MPA, mycophenolic acid; MMF, mycophenolate mofetil; TFP, trifluoperazine.

3-*O*-glucuronide. Trifluoperazine (TFP), which is one of the antischizophrenic agents, is metabolized as *N*-glucuronide by human UGT1A4 (Uchaipichat et al., 2006).

In drug development, experimental animals are frequently used for pharmacokinetic studies. The investigation of species differences in drug metabolism is essential for understanding the results of in vivo animal studies. However, there is insufficient information on species differences in glucuronidation. The purpose of the present study was to clarify the species differences in mouse and rat UGT activities in intestine and liver using seven typical substrates (estradiol, 4-MU, 4-NP, MPA, propofol, morphine, and TFP).

Materials and Methods

Materials. UDPGA, alamethicin, aprotinin, bestatin, leupeptin, trypsin inhibitor (type II-S: soybean), estradiol, estradiol 3-*O*-glucuronide, 4-MU, 4-MU *O*-glucuronide, and 4-NP *O*-glucuronide were purchased from Sigma-Aldrich (St. Louis, MO). (*p*-Amidinophenyl)methanesulfonyl fluoride, MPA, 4-NP, and TFP were obtained from Wako Pure Chemicals (Osaka, Japan). Morphine hydrochloride was purchased from Takeda Pharmaceutical Company (Osaka, Japan). Morphine 3-*O*-glucuronide was kindly provided by Dr. Kazuta Oguri (Kyusyu University, Fukuoka, Japan). MPA *O*-glucuronide and carboxybutoxy ether of mycophenolic acid were generous gifts from Roche Bioscience (Palo Alto, CA). All other chemicals and solvents were of analytical grade or the highest grade commercially available.

Preparation of Intestinal and Hepatic Microsomes. C57BL/6J mice (7-week-old male, 21–26 g, and female, 17–20 g), BALB/c, C3H/HeJ, DBA/2, ddY, and ICR mice (7-week-old male, 21–34 g), and Sprague-Dawley rats (7-week-old male, 220–240 g, and female, 140–160 g) were obtained from SLC Japan (Hamamatsu, Japan). Animals were housed in the institutional animal facility in a controlled environment (temperature 25 ± 1°C and 12-h light/dark cycle) with access to food and water ad libitum. Animals were acclimatized for a week before use. Animal were maintained in accordance with the National Institutes of Health Guide for Animal Welfare of Japan, as approved by the Institutional Animal Care and Use Committee of Kanazawa University.

Pooled duodenal, jejunal, iliac, and colonic microsomes from five mice or rats were prepared according to the method of Emoto et al. (2000) with slight modifications. Briefly, duodenum, jejunum, ileum, and colon were divided, cut longitudinally, and then washed in ice-cold 1.15% KCl by gentle swirling. The intestine was suspended in 3 vol of ice-cold buffer A [50 mM Tris-HCl buffer (pH 7.4) containing 150 mM KCl, 20% (v/v) glycerol, 1 mM EDTA, 1 mM (*p*-amidinophenyl)methanesulfonyl fluoride, 1 mg/ml trypsin inhibitor, 10 μM leupeptin, 0.04 U/ml aprotinin, and 1 μM bestatin] and homogenized using a motor-driven Teflon-tipped pestle. The homogenate was centrifuged at 9000*g* at 4°C for 20 min, and then the supernatant was centrifuged at 105,000*g* at 4°C for 60 min. The microsomal pellets were resuspended in ice-cold buffer A.

Pooled hepatic microsomes from five mice or rats were prepared according to the method described by Emoto et al. (2000). Protein concentrations were determined according to the method of Lowry et al. (1951) using bovine serum albumin as the standard.

Enzyme Assays. A typical incubation mixture contained 50 mM Tris-HCl buffer (pH 7.4), 5 mM $MgCl_2$ (except propofol and TFP, 10 mM), 25 μg/ml alamethicin, UDPGA, microsomes, and a substrate. In the preliminary study, the concentration of UDPGA was confirmed to reach a plateau level for each UGT activity. Microsomes with alamethicin were placed on ice for 15 min. In the preliminary study, a change of preincubation time did not affect the UGT activities. The final concentration of methanol (estradiol and propofol) or ethanol (MPA) in the reaction mixture was <1.5% (v/v). As described by Uchaipichat et al. (2004), because methanol (>1%) decreased more than 20% of the UGT1A6 activity, the final concentrations of methanol for 4-MU and 4-NP *O*-glucuronidation were <0.75% and <0.5% (v/v), respectively. A portion of the sample was subjected to high-performance liquid chromatography. The flow rate was 1.0 ml/min.

Estradiol 3-*O*-glucuronidation was determined according to the method of Yoon et al. (2003) with slight modifications. In the preliminary study, the rate of this activity was linear with respect to the microsomal protein concentrations (<0.1 mg/ml in mice and <0.05 mg/ml in rats) and incubation time (<15 min in mice and <30 min in rats). Therefore, in both mice and rats, the concentrations of microsomal protein were 0.05 mg/ml, and the reaction mixture was incubated for 15 min. The concentrations of UDPGA were 3 (mice) and 7 mM (rats). The analytical column was a TSKgel ODS-80Ts (4.6 × 150 mm, 5 μm; TOSOH, Tokyo, Japan), and the mobile phase was acetonitrile-1 mM perchloric acid (25:75, v/v).

4-MU *O*-glucuronidation was determined according to the method of Uchaipichat et al. (2004) with slight modifications. In the preliminary study, the rate of this activity was linear with respect to the microsomal protein concentrations (<0.2 mg/ml in mice and <0.1 mg/ml in rats) and incubation time (<30 min in mice and <15 min in rats). In the reaction mixture, the concentrations of microsomal protein were 0.1 (mice) and 0.05 mg/ml (rats). In both mice and rats, the concentration of UDPGA was 3 mM, and the reaction mixture was incubated for 15 min. The analytical column was a CAPCEL PAK C_{18} UG120 (4.6 × 150 mm, 5 μm; Shiseido, Tokyo, Japan), and the mobile phase was methanol-50 mM potassium phosphate buffer, pH 4.5 (20:80, v/v).

4-NP *O*-glucuronidation was determined according to the method of Hanioka et al. (2001) with slight modifications. In the preliminary study, the rate of this activity was linear with respect to the microsomal protein concentrations (<0.2 mg/ml in both mice and rats) and incubation time (<30 min in mice and <15 min in rats). In the reaction mixture, the concentrations of microsomal protein were 0.1 (mice) and 0.05 mg/ml (rats). In both mice and rats, the concentration of UDPGA was 3 mM, and the reaction mixture was incubated for 15 min. The analytical column was a Mightysil RP-18 (4.6 × 150 mm, 5 μm; Kanto Chemical, Tokyo, Japan), and the mobile phase was methanol-50 mM potassium phosphate buffer, pH 6.5 (6:94, v/v).

Propofol *O*-glucuronidation was determined according to the method of Fujiwara et al. (2007) with slight modifications. In the preliminary study, the rate of this activity was linear with respect to the microsomal protein concentrations (<0.25 mg/ml in mice and <1.0 mg/ml in rats) and incubation time (<30 min in mice and <45 min in rats). In the reaction mixture, the concentrations of microsomal protein were 0.25 (mice) and 0.5 mg/ml (rats). In both mice and rats, the concentration of UDPGA was 5 mM, and the reaction mixture was incubated for 30 min (mice) and 45 min (rats). The analytical column was a Mightysil RP-18 (4.6 × 150 mm, 5 μm), and the mobile phase was acetonitrile-0.1% acetic acid (40:60, v/v).

MPA *O*-glucuronidation was determined according to the method of Picard et al. (2005). In the preliminary study, the rate of this activity was linear with respect to the microsomal protein concentrations (<0.2 mg/ml in mice and <0.5 mg/ml in rats) and incubation time (<45 min in mice and <60 min in rats). In the reaction mixture, the concentrations of microsomal protein were 0.1 (mice) and 0.2 mg/ml (rats) and the concentration of UDPGA was 7 (mice) and 3 mM (rats). The reaction mixture was incubated for 30 min. Carboxybutoxy ether of mycophenolic acid (4.6 nmol) was added as an internal standard. The analytical column was an Inertsil ODS-3 (4.6 × 250 mm, 5 μm; GL Sciences, Tokyo, Japan), and the mobile phase was acetonitrile-0.1% phosphoric acid (30:70, v/v).

Morphine 3-*O*-glucuronidation was determined according to the method of Katoh et al. (2005) with slight modifications. In the preliminary study, the rate of this activity was linear with respect to the microsomal protein concentrations (<1.0 mg/ml in mice and <0.2 mg/ml in rats) and incubation time (<105 min in mice and <30 min in rats). In both mice and rats, the concentrations of UDPGA and microsomal protein were 10 mM and 0.2 mg/ml, respectively. The reaction mixture was incubated for 90 min (mice) and 30 min (rats). The analytical column was a Develosil C30-UG-5 (4.6 × 150 mm, 5 μm; Nomura Chemical, Aichi, Japan) and the mobile phase was 50 mM sodium dihydrogen phosphate.

TFP *N*-glucuronidation was determined according to the method of Uchaipichat et al. (2006) with slight modifications. The concentrations of UDPGA and microsomal protein were 2.5 mM and 0.25 mg/ml, respectively. The reaction mixture was incubated for 30 min. The analytical column was an Inertsil ODS-3 (4.6 × 150 mm), and the mobile phase was acetonitrile-0.1% trifluoroacetic acid (30:70, v/v).

Kinetic Analyses. The kinetic studies were performed using pooled liver microsomes of C57BL/6J mouse, pooled duodenal microsomes of C57BL/6J mouse, pooled rat liver microsomes, and pooled rat duodenal microsomes. When the kinetic parameters were determined, the concentrations of estradiol, 4-MU, 4-NP, propofol, MPA, and morphine ranged from 5 to 150, 10 to 640,

TABLE 1

Kinetic parameters of UGT activities in liver microsomes from male and female mice and rats

TFP *N*-glucuronide was not detected in liver microsomes from male and female mice and rats.

Substrate	Species	Sex	K_m (S_{50})	V_{max}	K_{si}	CL_{int} (CL_{max})	n^a
			μM	*nmol/min/mg protein*	*μM*	*μl/min/mg protein*	
Estradiol	Mouse	M	17 ± 3[b]	6.1 ± 0.3		179[c]	2.3
		F	18 ± 2[b]	6.6 ± 0.4		183[c]	2.3
	Rat	M	16 ± 3[b]	6.1 ± 0.4		193[c]	1.8
		F	16 ± 2[b]	7.1 ± 0.3		231[c]	1.8
4-MU	Mouse	M	71 ± 8[b]	214 ± 9		1975[c]	1.2
		F	59 ± 3[b]	159 ± 3		1436[c]	1.5
	Rat	M	130 ± 11[b]	264 ± 11		1146[c]	1.4
		F	130 ± 6[b]	286 ± 7		1241[c]	1.3
4-NP	Mouse	M	116 ± 23	40 ± 2		341	
		F	112 ± 24	33 ± 2		293	
	Rat	M	378 ± 73	81 ± 7		213	
		F	635 ± 108	73 ± 6		115	
Propofol	Mouse	M	31 ± 3	1.9 ± 0.1	1069 ± 96	62	
		F	51 ± 11	2.5 ± 0.3	514 ± 105	49	
	Rat	M	16 ± 4	0.22 ± 0.07		14	
		F	51 ± 21	0.06 ± 0.01		1.2	
MPA	Mouse	M	307 ± 59	24 ± 2		78	
		F	242 ± 21	27 ± 1		111	
	Rat	M	344 ± 26	5.9 ± 0.2		17	
		F	304 ± 24	3.0 ± 0.1		9.9	
Morphine	Mouse	M	421 ± 17	19 ± 0		46	
		F	318 ± 15	20 ± 0		64	
	Rat	M	1406 ± 17	39 ± 0		27	
		F	1319 ± 79	35 ± 1		26	

[a] Hill coefficient.
[b] S_{50}.
[c] CL_{max}.

10 to 1000 (10 to 1500 in mouse duodenum), 5 to 2000, 10 to 1000, and 20 to 6000 μM, respectively. The kinetic parameters and S.E.s were estimated from the fitted curves using a computer program (KaleidaGraph; Synergy Software, Reading, PA) designed for nonlinear regression analysis. The following equations were used: Michaelis-Menten equation, $V = V_{max} \cdot [S]/(K_m + [S])$; Hill equation, $V = V_{max} \cdot [S]^n/(S_{50}{}^n + [S]^n)$; and substrate inhibition equation, $V = V_{max} \cdot [S]/(K_m + [S] + [S]^2/K_{si})$, where V is the velocity of the reaction, S is the substrate concentration, K_m is the Michaelis-Menten constant, V_{max} is the maximum velocity, S_{50} is the substrate concentration showing the half-V_{max}, n is the Hill coefficient, and K_{si} is the substrate inhibition constant. Intrinsic clearance (CL_{int}) was calculated as V_{max}/K_m for Michaelis-Menten kinetics. For sigmoidal kinetics, maximum clearance (CL_{max}) was calculated as $V_{max} \cdot (n - 1)/(S_{50} \cdot n(n - 1)^{1/n})$ to estimate the highest clearance (Houston and Kenworthy, 2000). In the present study, if the Hill coefficient was more than 1.2, the kinetic data were fit to the Hill equation.

UGT Activities in Intestine. The UGT activities were determined using pooled duodenal, jejunal, ileal, and colonic microsomes from C57BL/6J mice or rats. The concentrations of estradiol, 4-MU, 4-NP, propofol, MPA, and morphine were 20, 100, 300, 60, 200, and 200 μM, respectively, which were the concentrations below apparent K_m values in duodenal microsomes from mice or rats. Other experimental conditions were the same as described above. For investigation of strain differences in mice, the UGT activities were determined in pooled duodenal and liver microsomes from six strains using six substrates.

Results

Kinetic Analyses of UGT Activities in Mouse and Rat Liver Microsomes Using Seven UGT Substrates. To investigate species and sex differences, kinetic analyses of estradiol 3-*O*-, 4-MU *O*-, 4-NP *O*-, propofol *O*-, MPA *O*-, morphine 3-*O*-, and TFP *N*-glucuronidation were determined in liver microsomes from male mice, female mice, male rats, and female rats. When kinetic parameters were determined, the concentrations of estradiol, 4-MU, 4-NP, propofol, MPA, and morphine ranged from 5 to 150, 10 to 640, 10 to 1000, 5 to 2000, 10 to 1000, and 20 to 6000 μM, respectively. Kinetic parameters are shown in Table 1. In all kinetic analyses, the r values for fitting to the kinetic model were more than 0.97. The estradiol 3-*O*-glucuronidation in all liver microsomes was fitted to the Hill equation. The Hill coefficient in both male and female mice (2.3) was higher than that in both male and female rats (1.8). The 4-MU *O*-glucuronidation in all liver microsomes was fitted to the Hill equation. Kinetic parameters were different between mice and rats. The 4-NP *O*-glucuronidation in all liver microsomes was fitted to the Michaelis-Menten kinetics. The propofol *O*-glucuronidation in male and female mouse liver microsomes was fitted to the substrate inhibition kinetics, whereas those in male and female rat liver microsomes were fitted to the Michaelis-Menten kinetics. The MPA *O*-glucuronidation in all liver microsomes was fitted to the Michaelis-Menten kinetics. In females, species differences in the apparent K_m and V_{max} values were observed as in males. The morphine 3-*O*-glucuronidation in all liver microsomes was fitted to the Michaelis-Menten kinetics. The TFP *N*-glucuronidation in male mouse and male rat liver microsomes was measured. However, this activity was not detected in either mice or rats.

Microsomal UGT Activities in Duodenum, Jejunum, Ileum, and Colon from Mice and Rats. UGT activities using six different substrates were measured in microsomes prepared from male and female mouse and rat duodenum, jejunum, ileum, and colon (Fig. 1). In male mice, 4-NP *O*- and morphine 3-*O*-glucuronidation in colon were higher than those in other parts of the intestine, whereas estradiol 3-*O*-, 4-MU *O*-, and propofol *O*-glucuronidation in duodenum were higher than those in other parts of the intestine. In male rats, the duodenum exhibited higher activities of 4-NP, propofol, MPA, and morphine glucuronidation than those in other parts of the intestine. In female rats, all UGT activities except morphine were decreased distally through the intestine. In all parts of the intestine, 4-MU *O*-, 4-NP *O*-, and morphine 3-*O*-glucuronidation in mice were lower than those in rats.

DRUG METABOLISM AND DISPOSITION DMD aspet

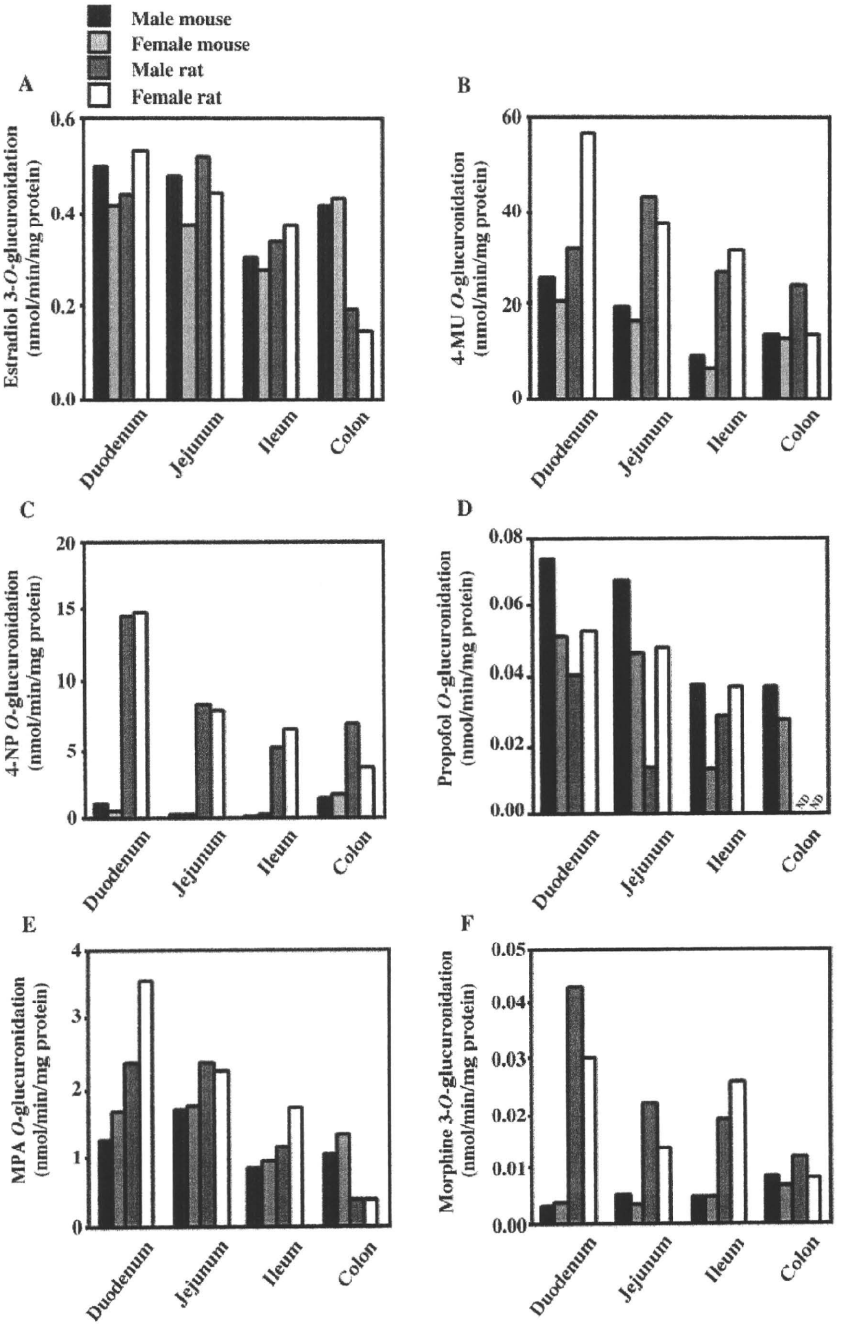

FIG. 1. UGT activities in duodenal, jejunal, ileal, and colonic microsomes from C57BL/6 mice and Sprague-Dawley rats. The formations of estradiol 3-*O*-glucuronide (A), 4-MU *O*-glucuronide (B), 4-NP *O*-glucuronide (C), propofol *O*-glucuronide (D), MPA *O*-glucuronide (E), and morphine 3-*O*-glucuronide (F) were determined as described under *Materials and Methods*. The concentrations of estradiol, 4-MU, 4-NP, propofol, MPA, and morphine were 20, 100, 300, 60, 200, and 200 μM, respectively. Each column represents the mean of duplicate determinations. ND, not detected.

Kinetic Analyses of UGT Activities in Duodenal Microsomes from Male Mice and Rats Using Seven UGT Substrates. Kinetic analyses of estradiol 3-*O*-, 4-MU *O*-, 4-NP *O*-, propofol *O*-, MPA *O*-, morphine 3-*O*-, and TFP *N*-glucuronidation in microsomes from male mice and rats were determined. Kinetic parameters are shown in Table 2. The estradiol 3-*O*-glucuronidation in duodenal microsomes from mice was fitted to the Hill equation. In comparison with liver, the CL_{max} values in duodenum were 6.5-fold lower. The Hill coefficient in duodenum was also lower than that in liver. On the other hand, this activity in rat duodenal microsomes was fitted to the Michaelis-Menten equation rather than to the Hill equation. When the kinetic data from rat duodenal microsomes were fit to the Hill equation, the S_{50} value, the V_{max} value, and the Hill coefficient were 29 μM, 1.2 nmol/min/mg protein, and 1.1, respectively. The 4-MU *O*-glucuronidation in duodenal microsomes from male mice and rats was fitted to the Michaelis-Menten equation. The 4-NP *O*-glucuronidation in duodenal microsomes from male mice did not reach a plateau level up to 1500 μM. In rat duodenal microsomes, this activity was fitted to the Michaelis-Menten kinetics with lower K_m values than in mice. The propofol *O*-glucuronidation in duodenal microsomes showed substrate inhibition at substrate concentrations >400 μM in male mice and >500 μM in female rats, but the plot did not fit to either the substrate inhibition kinetics or the two-site model used by Houston and Kenworthy (2000). Therefore, we did not calculate the kinetic parameters for propofol *O*-glucuronidation in duodenal microsomes. The MPA *O*-glucuronidation in duodenal microsomes from both male mice and rats was fitted to

TABLE 2

Kinetic parameters of UGT activities in duodenal microsomes from male mice and rats

TFP *N*-glucuronide was not detected in microsomes from male mice and rats.

Substrate	Species	K_m (S_{50})	V_{max}	CL_{int} (CL_{max})	n^a
		μM	*nmol/min/mg protein*	*μl/min/mg protein*	
Estradiol	Mouse	42 ± 7[b]	2.2 ± 0.2	28[c]	1.6
	Rat	35 ± 10	1.3 ± 0.1	38	
4-MU	Mouse	164 ± 46	63 ± 7	387	
	Rat	416 ± 19	190 ± 4	458	
4-NP	Mouse	>1500			
	Rat	494 ± 117	33 ± 4	67	
MPA	Mouse	1272 ± 349	8.9 ± 1.6	7.0	
	Rat	340 ± 47	6.7 ± 0.4	20	
Morphine	Mouse	2380 ± 103	0.05 ± 0.00	0.02	
	Rat	320 ± 23	0.11 ± 0.00	0.34	

[a] Hill coefficient.
[b] S_{50}.
[c] CL_{max}.

the Michaelis-Menten kinetics. The CL_{int} value in mouse duodenum was 11-fold lower than that in liver. However, in rats, that value in duodenum (20 μl/min/mg protein) was similar to the value in liver (17 μl/min/mg protein). The morphine 3-*O*-glucuronidation in duodenal microsomes from both male mice and rats was fitted to the Michaelis-Menten kinetics. The CL_{int} value in mouse duodenum was lower than that in liver. The TFP *N*-glucuronidation in mouse and rat duodenal microsomes was determined. As in liver, these activities in both mice and rats were not detected.

Strain Differences of UGT Activities in Mouse Duodenal Microsomes. To investigate the strain differences in mice, the UGT activities using six UGT substrates were determined in duodenal microsomes from C57BL/6J, BALB/c, C3H/HeJ, DBA/2, ddY, and ICR mice (Fig. 2). For all UGT activities except 4-MU, C3H/HeJ mice showed the highest values among the six strains. The UGT activities in BALB/c and C3H/HeJ mice were relatively high compared with those in other mice. The UGT activities in the six strains showed a similar tendency between 4-NP *O*- and MPA *O*-glucuronidation or between estradiol 3-*O*- and propofol *O*-glucuronidation. The strain differences in UGT activities varied according to the substrates. Conversely, in liver, there was not much difference in UGT activities among the six mouse strains (Table 3).

Discussion

Information on species differences in UGT activities is insufficient. Intestine as well as liver plays an important role in xenobiotic metabolism. Numerous phase I and phase II drug-metabolizing enzymes are expressed in intestine. Recently, species differences in glucuronidation of the anti-human immunodeficiency virus drug bevirimat were reported (Wen et al., 2007). However, there have been no comprehensive analyses of UGT activities in intestine and liver from mice and rats. In the present study, kinetic analyses of UGT activities using seven typical substrates (estradiol, 4-MU, 4-NP, propofol, MPA, morphine, and TFP) in intestine and liver microsomes from mice and rats were investigated. In addition, strain differences in UGT activities in mouse duodenum were studied.

Estradiol 3-*O*-glucuronidation is catalyzed mainly by human UGT1A1. Rat UGT1A1 is responsible for this reaction (King et al., 1996). In human liver microsomes, estradiol 3-*O*-glucuronosyltransferase yielded an S_{50} value of 17 μM, and a Hill coefficient of 1.8 (Fisher et al., 2000a). The S_{50} value was almost the same among three species. In microsomes from humans, the estradiol 3-*O*-glucuronidation in small intestine was higher than that in liver as reported by Fisher et al. (2000b), which was contrary to the present results in mice and rats. In the present study, the CL_{max} value for estradiol 3-*O*-glucuronidation in female rats was higher than that in male rats. For glucuronidation of bilirubin, another UGT1A1 substrate, sex differences in Wistar rats have been clarified (Muraca and Fevery, 1984). However, the sex differences in UGT1A1 activity are still unclear.

UGT1A6 is a major enzyme catalyzing the glucuronidation of various simple phenolic compounds such as 4-MU and 4-NP in the liver. UGT1A6 is likely to be functionally orthologous among several species including humans, rats, mice, and rabbits (Iyanagi et al., 1986; Harding et al., 1988; Lamb et al., 1994). The 4-MU glucuronidation in human liver microsomes followed the Michaelis-Menten kinetics (Miners et al., 1988) and was catalyzed by several human UGTs (Uchaipichat et al., 2004). The different kinetic models between humans and rodents might be due to the different UGT enzymes. In duodenum, the apparent K_m value for 4-NP glucuronidation in mice was higher than that in rats, suggesting that the affinity of 4-NP to mouse Ugt may be lower than that to rat UGT. In contrast, in liver, the apparent K_m value in mice was lower than that in rats. In the case of other UGT1A6 substrates, the hepatic serotonin *O*-glucuronidation in Wistar rats was higher than that in CD-1 mice (Krishnaswamy et al., 2003), whereas the hepatic acetaminophen *O*-glucuronidation in Wistar rats was lower than that in CD-1 mice (Court, 2001).

Rat *UGT1A9* is a pseudogene, but human *UGT1A9* and mouse *Ugt1a9* are not. The glucuronidation of propofol is catalyzed by human UGT1A8 (Mano et al., 2004) and by human UGT1A9 in the liver (Court, 2005) in a manner consistent with the substrate inhibition kinetics (Fujiwara et al., 2007). In the present study, the glucuronidation of propofol in liver microsomes from both male and female mice was fitted to the substrate inhibition kinetics, whereas those in other microsomes were not fit. These differences in the kinetic profile may be accounted for by the absence of UGT1A9 protein in rats. Propofol *O*-glucuronidation may be catalyzed by other UGTs, possibly UGT1A8, in rats.

MPA is the active metabolite of MMF, which induces gastrointestinal toxicity. Stern et al. (2007) reported that female rats were more susceptible to MMF-induced gastrointestinal toxicity than male rats, because of the fact that female rats showed lower intestinal MPA *O*-glucuronidation than male rats. In the present study, in duodenum the CL_{int} value for the MPA *O*-glucuronide formation in male mice was lower than that in male rats. This result suggests that male mice may be more susceptibility to MMF-induced gastrointestinal toxicity than male rats. Human UGT1A9 is mainly involved in hepatic MPA *O*-glucuronidation (Bernard and Guillemette, 2004). Picard et al. (2005) reported that in microsomes from humans the CL_{int} value in

DRUG METABOLISM AND DISPOSITION DMD aspet

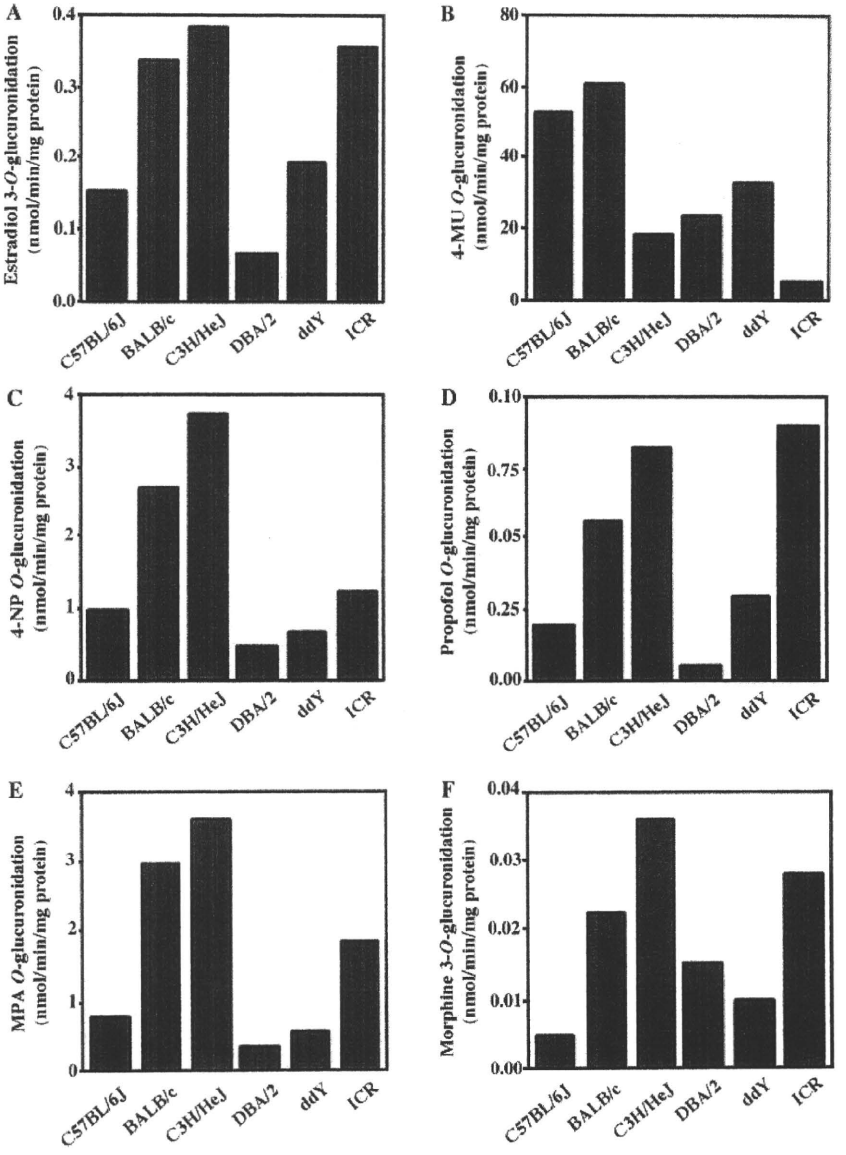

FIG. 2. UGT activities in duodenal microsomes from male C57BL/6J, BALB/c, C3H/HeJ, DBA/2, ddY, and ICR mice. The formations of estradiol 3-*O*-glucuronide (A), 4-MU *O*-glucuronide (B), 4-NP *O*-glucuronide (C), propofol *O*-glucuronide (D), MPA *O*-glucuronide (E), and morphine 3-*O*-glucuronide (F) were determined as described under *Materials and Methods*. The concentrations of estradiol, 4-MU, 4-NP, propofol, MPA, and morphine were 20, 100, 300, 60, 200, and 200 μM, respectively. Each column represents the mean of duplicate determinations.

TABLE 3

UGT activities in liver microsomes from the six mouse strains

Data represent the mean of duplicate determinations. The concentrations of estradiol, 4-MU, 4-NP, propofol, MPA, and morphine were 20, 100, 300, 60, 200, and 200 μM, respectively.

Strain	UGT Activities					
	Estradiol	4-MU	4-NP	Propofol	MPA	Morphine
	nmol/min/mg protein					
C57BL/6J	0.89	147	46	1.7	17	8.4
BALB/c	0.77	199	71	1.2	14	8.5
C3H/HeJ	0.79	169	62	1.7	17	8.4
DBA/2	0.82	133	56	3.5	28	8.2
ddY	0.80	160	63	3.5	25	8.3
ICR	0.71	136	65	3.3	26	8.6

liver (28.7 μl/min/mg protein) was higher than that in intestine (0.7 μl/min/mg protein). In the present study in mice, the CL_{int} value in liver was higher than that in duodenum, but mouse Ugt catalyzing MPA *O*-glucuronidation has not been determined yet. Rat UGT1A7 is mainly involved in MPA *O*-glucuronidation (Miles et al., 2005, 2006). In the present study, the CL_{int} value in rats was similar in liver and duodenum and may be catalyzed by UGT1A7.

In humans, approximately 55% of morphine is metabolized into morphine 3-*O*-glucuronide and approximately 15% into morphine 6-*O*-glucuronide (Milne et al., 1996). The ratios of morphine 3-*O*-